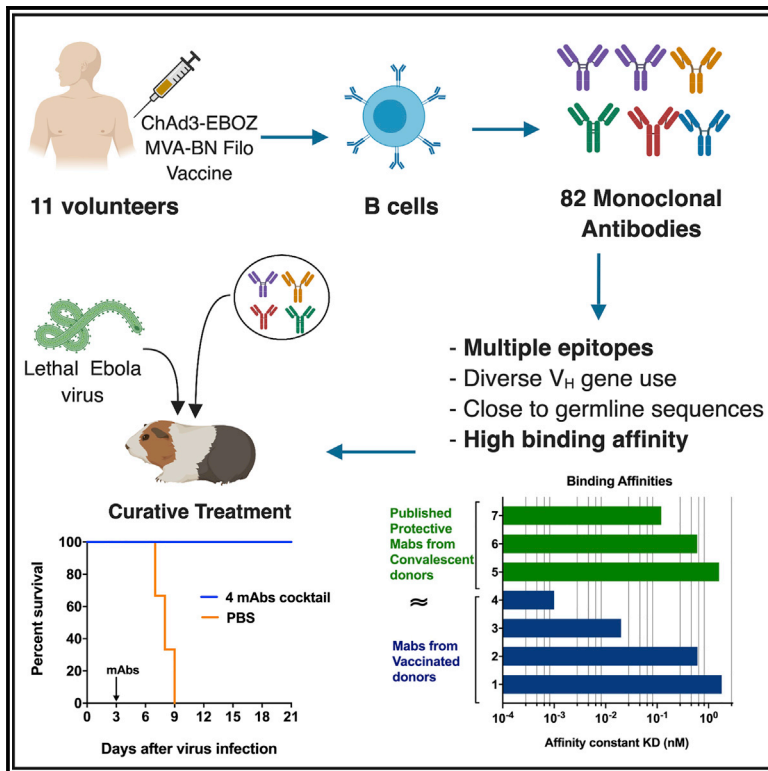


Cell Reports

Therapeutic Monoclonal Antibodies for Ebola Virus Infection Derived from Vaccinated Humans

Graphical Abstract



Authors

Pramila Rijal, Sean C. Elias, Samara Rosendo Machado, ..., Daniel J. Lightwood, Simon J. Draper, Alain R. Townsend

Correspondence

pramila.rijal@rdm.ox.ac.uk (P.R.), alain.townsend@imm.ox.ac.uk (A.R.T.)

In Brief

Most antibodies used for Ebola virus treatment originate from convalescent donors or highly immunized animals. Rijal et al. find that monoclonal antibodies isolated early after vaccination from humans can be powerfully therapeutic, despite the relative immaturity of their sequences. Vaccine trials therefore can provide a valuable source of therapeutic antibodies.

Highlights

- Therapeutic antibodies for Ebola were isolated from human donors in a vaccine trial
- The derived antibodies were close to germline in sequence
- Despite temporal immaturity, their binding kinetics matched established antibodies
- Vaccine trials can provide a golden opportunity to isolate therapeutic antibodies



Therapeutic Monoclonal Antibodies for Ebola Virus Infection Derived from Vaccinated Humans

Pramila Rijal,^{1,*} Sean C. Elias,² Samara Rosendo Machado,¹ Julie Xiao,¹ Lisa Schimanski,¹ Victoria O'Dowd,³ Terry Baker,³ Emily Barry,³ Simon C. Mendelsohn,² Catherine J. Cherry,² Jing Jin,² Geneviève M. Labbé,² Francesca R. Donnellan,² Tommy Rampling,² Stuart Dowall,⁴ Emma Rayner,⁴ Stephen Findlay-Wilson,⁴ Miles Carroll,⁴ Jia Guo,⁵ Xiao-Ning Xu,⁵ Kuan-Ying A. Huang,⁶ Ayato Takada,⁷ Gillian Burgess,³ David McMillan,³ Andy Popplewell,³ Daniel J. Lightwood,³ Simon J. Draper,² and Alain R. Townsend^{1,8,*}

¹MRC Human Immunology Unit, MRC Weatherall Institute of Molecular Medicine, Radcliffe Department of Medicine, University of Oxford, Oxford OX3 9DS, UK

²Jenner Institute, University of Oxford, Old Road Campus Research Building, Oxford OX3 7DQ, UK

³UCB Pharma, Slough SL1 3WE, UK

⁴Public Health England, Porton Down, Wiltshire, UK

⁵Centre for Immunology and Vaccinology, Chelsea & Westminster Hospital, Faculty of Medicine, Imperial College, London, UK

⁶Division of Paediatric Infectious Diseases, Department of Paediatrics, Chang Gung Memorial Hospital, Taoyuan, Taiwan

⁷Division of Global Epidemiology, Research Center for Zoonosis Control, Hokkaido University, Sapporo, Japan

⁸Lead Contact

*Correspondence: pramila.rijal@rdm.ox.ac.uk (P.R.), alain.townsend@imm.ox.ac.uk (A.R.T.)

<https://doi.org/10.1016/j.celrep.2019.03.020>

SUMMARY

We describe therapeutic monoclonal antibodies isolated from human volunteers vaccinated with recombinant adenovirus expressing Ebola virus glycoprotein (EBOV GP) and boosted with modified vaccinia virus Ankara. Among 82 antibodies isolated from peripheral blood B cells, almost half neutralized GP pseudotyped influenza virus. The antibody response was diverse in gene usage and epitope recognition. Although close to germline in sequence, neutralizing antibodies with binding affinities in the nano- to pico-molar range, similar to “affinity matured” antibodies from convalescent donors, were found. They recognized the mucin-like domain, glycan cap, receptor binding region, and the base of the glycoprotein. A cross-reactive cocktail of four antibodies, targeting the latter three non-overlapping epitopes, given on day 3 of EBOV infection, completely protected guinea pigs. This study highlights the value of experimental vaccine trials as a rich source of therapeutic human monoclonal antibodies.

INTRODUCTION

The Ebola virus (EBOV) outbreak in 2013–2016 in West Africa resulted in 28,616 cases and 11,310 deaths (<https://www.who.int/csr/disease/ebola/en/>). A new outbreak in 2018 is in progress in the Democratic Republic of Congo, which has claimed 528 lives to date (<https://www.who.int/ebola/situation-reports/drc-2018/en/>). During the 2013–2016 outbreak, there were no approved vaccines or therapeutics, only experimental ones. ZMapp anti-

bodies were tested in human trials during the outbreak in West Africa. Although the ZMapp cocktail was not proven statistically to be protective because of the small number of participants, there was a trend in the direction of improved survival (Davey et al., 2016). The ZMapp cocktail of murine chimeric antibodies (c13C6, c2G4, and c4G7), one targeting the glycan cap and two to the base of the glycoprotein, was successful in protecting 100% of non-human primates as late as 5 days post infection (Qiu et al., 2014).

Mixtures of monoclonal antibodies to the EBOV glycoprotein (GP) from convalescent humans (Maruyama et al., 1999; Flyak et al., 2016, 2018; Corti et al., 2016; Bornholdt et al., 2016; Wec et al., 2017; Gilchuk et al., 2018), humanized mice (Pascal et al., 2018), hyper-immunized macaques (Keck et al., 2015; Zhao et al., 2017), and wild-type mice (Furuyama et al., 2016; Marzi et al., 2012; Wilson et al., 2000; Qiu et al., 2012; Pettitt et al., 2013; Takada et al., 2007) have been shown to be therapeutic in various animal models. The antibodies of human origin, 114 (to the receptor binding region) and 100 (to the base), showed a similarly profound therapeutic effect (Corti et al., 2016). Another new cocktail from Regeneron, derived from humanized mice, containing one antibody to the fusion loop, one to the head, and one to the glycan cap was also protective in primates at a dose of 150 mg/Kg (Pascal et al., 2018) and has recently been approved for emergency experimental use during the 2018 outbreak in the Democratic Republic of Congo. This cocktail was intentionally chosen to combine antibodies to independent epitopes with neutralization and immune effector functions, thought to be complementary. However, none of these therapeutic cocktails are cross-protective to the other species of Ebola that can cause human disease. These results encourage the development of optimized cocktails of antibodies for use against human disease caused by the complete range of Ebola virus species.

A recent comprehensive study of monoclonal antibodies collected from laboratories across the globe by the Viral



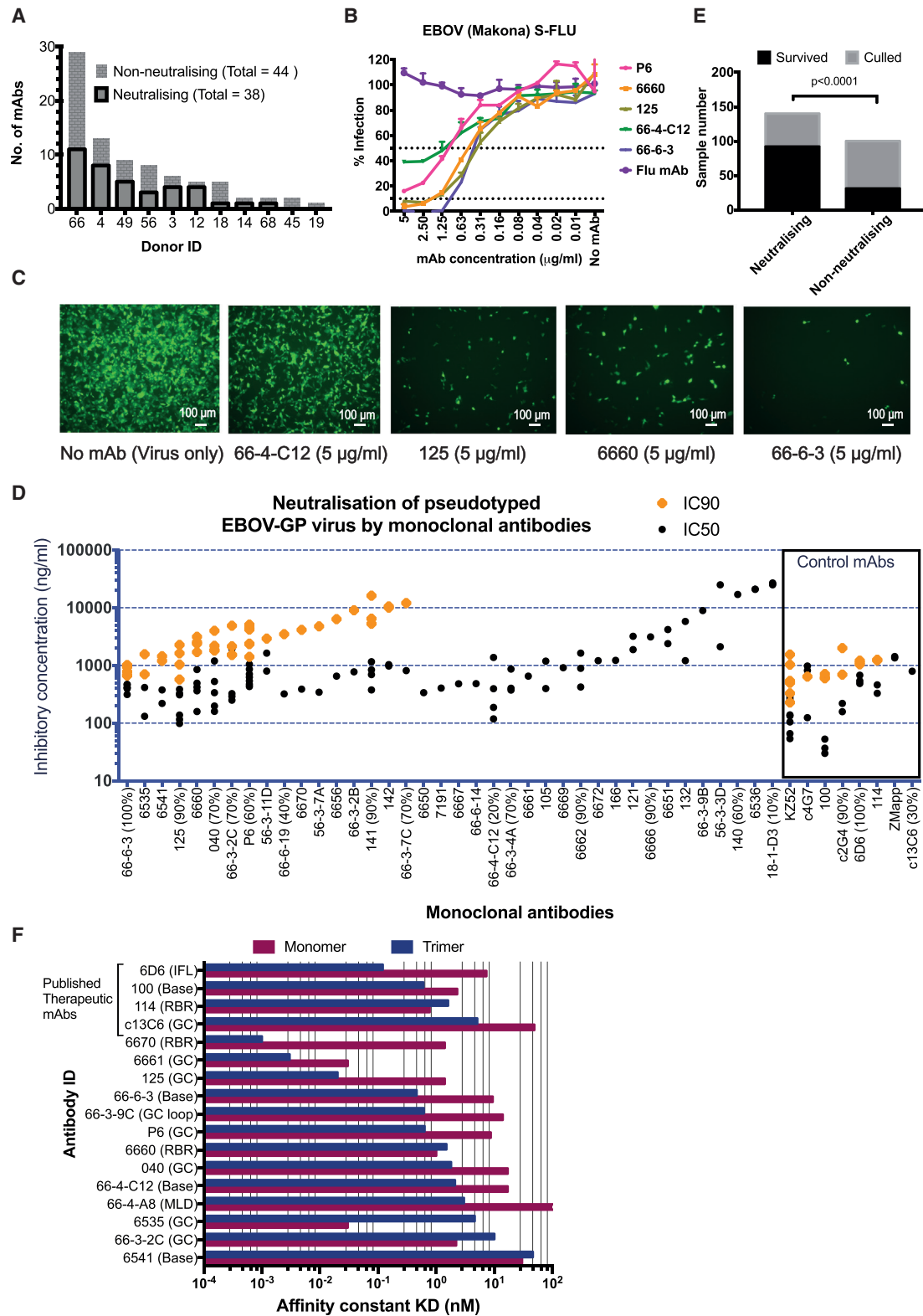


Figure 1. Human Monoclonal Antibodies Isolated from Vaccinated Individuals

(A) Total of 82 antibodies were isolated from 11 vaccinated volunteers. 38 out of 82 antibodies blocked infection of MDCK-SIAT1 cells by E-S-FLU.

(B) Example of *in vitro* microneutralization of Ebola pseudotyped influenza virus (named as E-S-FLU virus) infecting MDCK-SIAT1 cells.

(legend continued on next page)

Hemorrhagic Fever Immunotherapeutic Consortium (VIC) emphasized the variety of independent epitopes on the viral glycoprotein that can be bound by protective antibodies and the range of antibody-dependent mechanisms that can contribute to protection *in vivo* (Saphire et al., 2018). The VIC study established that neutralization *in vitro* was a strong indicator of the protective potential of an antibody but in addition, revealed that multiple Fc recruited functions also contributed to protection (Gunn et al., 2018). These results provided the theoretical background for our investigation.

In these examples, the great majority of therapeutic antibodies were isolated from animals or humans after multiple or prolonged exposures to the EBOV glycoprotein. These levels of exposure are thought to select for high-affinity antibodies through the acquisition of multiple adaptive somatic mutations after repeated rounds of competitive selection of B cells in the germinal centers of lymph nodes during affinity maturation; reviewed in (Eisen and Chakraborty, 2013; Oropallo and Cerutti, 2014). Structural analysis of human monoclonal antibodies to influenza hemagglutinin, isolated from each stage of this process, suggests that the useful mutations pre-configure the tertiary structure of the binding loops of the antibody to minimize the energy cost of binding. This can increase both the on-rate, and reduce the off-rate of the antibody to achieve affinities in the nano- to picomolar range associated with virus neutralization (Schmidt et al., 2013).

This explanatory framework suggests that antibodies with the required specificity and kinetics for neutralization may be present early in an immune response, but at a lower frequency than after full affinity maturation has taken place. If an efficient screening system is applied to finding them, antibodies with the required properties for therapy should be available from donors responding to an antigen for the first time. Human volunteers in experimental vaccine trials offer a convenient source of such antibodies without the difficulties of sample availability or concerns about persistent virus or other pathogens in venous samples from convalescent donors.

Here, we show that despite minimal affinity maturation, antibodies isolated from donors vaccinated with Ebola virus GP are as protective as antibodies from other sources in a rigorous test of therapy at day 3 of a lethal EBOV infection in the guinea pig model.

RESULTS

Isolation and Expression of Monoclonal Antibodies from Vaccinated Donors

Volunteers were vaccinated with ChAD3 EBOV (chimpanzee adenovirus 3 encoding EBOV glycoprotein) (Stanley et al.,

2014) and boosted with MVA-BN Filo, modified vaccinia virus Ankara (MVA) encoding the glycoproteins from EBOV Mayinga, SUDV Gulu and MARV (Marburg virus Musoke), and the nucleoprotein from TAFV produced by Bavarian Nordic (Ewer et al., 2016). A total of 82 antibodies were isolated from plasmablasts or memory B cells isolated at day 7 and day 28, respectively (Table S1), following booster vaccination with the MVA-BN-Filo from 11 vaccinated volunteers (Figure 1A, Table S5) as described in the STAR Methods.

Screening of Monoclonal Antibodies for Binding and Neutralization

MDCK-SIAT1 cells were transduced to express the glycoprotein from *Zaire ebolavirus* (H-sapiens-wt/GIN/2014/Kissidougou-C15) as described (Xiao et al., 2018). MDCK-SIAT1 cells were used in these experiments because, unlike other cell lines, they tolerate high levels of stable expression of EBOV GP, can pseudotype an influenza core, and are readily infected by our EBOV surrogate E-S-FLU (Xiao et al., 2018). Initial screening of antibodies was by detection of binding by indirect immunofluorescence to EBOV GP transduced cells.

GP-binding antibodies were then tested for blockade of infection of MDCK-SIAT1 cells by our Ebola surrogate E-S-FLU, which contains a disabled influenza core coated with Ebola GP. E-S-FLU encodes a fluorescent protein eGFP that replaces the hemagglutinin coding sequence so that infected cells fluoresce green. Thirty-eight of 82 antibodies inhibited infection by E-S-FLU as defined by loss of eGFP fluorescence after overnight infection by at least 50% (Figure 1D). We next distinguished “partially” neutralizing antibodies (inhibition of infection plateaus at 50%–90% inhibition) from “strongly” neutralizing monoclonal antibodies (mAbs) (that achieve $\geq 90\%$ inhibition of infection) as shown in Figure 1C. Figure 1D shows a summary of the 38 neutralizing antibodies compared to a set of control antibodies described in the literature including KZ52 (Maruyama et al., 1999; Lee et al., 2008), c4G7, c2G4, and c13C6—the three components of ZMapp (Murin et al., 2014), 100 and 114 (Corti et al., 2016; Misasi et al., 2016), and 6D6 (Furuyama et al., 2016).

The Relationship between *In Vitro* Neutralization and Protection *In Vivo* in Mice

A set of the first 24 antibodies isolated (14 showing $>50\%$ neutralization and 10 non-neutralizing) were tested for protection of mice (single dose of 100 μg at day 2 of infection with a mouse-adapted Ebola virus in groups of 10) as part of the work of the VIC (Saphire et al., 2018). This revealed that the 14 antibodies showing $>50\%$ neutralization in our assay provided overall 65.7% survival (range, 10%–100%), whereas the

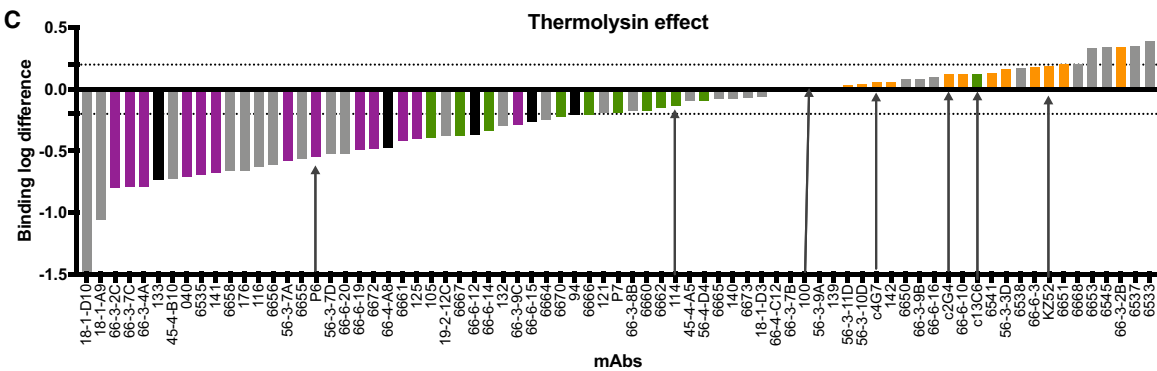
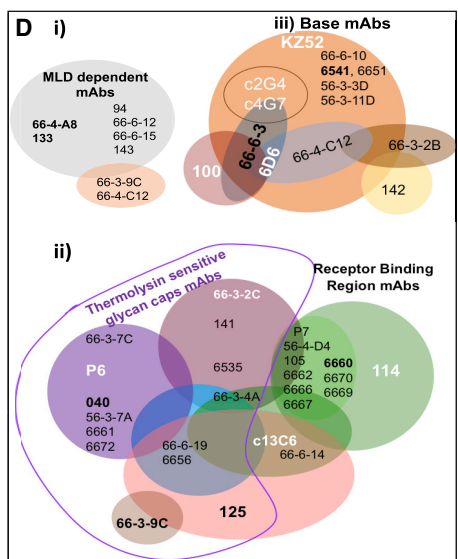
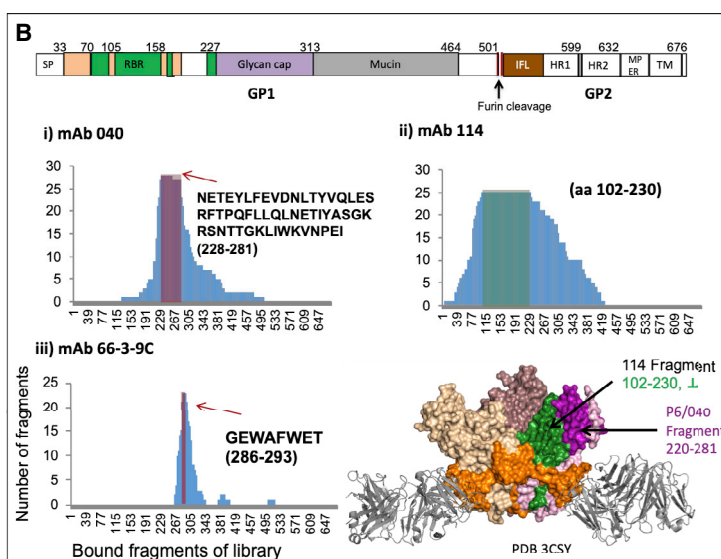
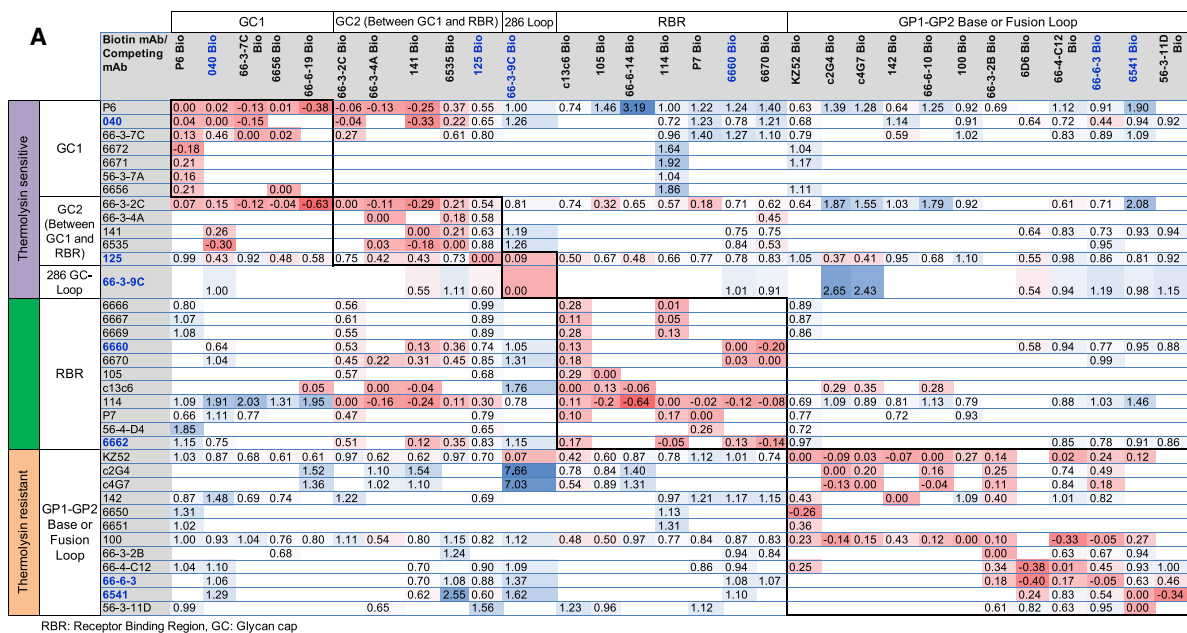
(C) Microscopic images showing virus neutralization by different antibodies at 5 $\mu\text{g}/\text{mL}$ concentration.

(D) *In vitro* neutralizing concentration of mAbs shown as IC_{50} and IC_{90} . Neutralization IC_{50} ranges from 0.1 to 10 $\mu\text{g}/\text{mL}$. Partially neutralizing antibodies have no IC_{90} values. Almost half of the antibodies have titers comparable to that of the antibodies published in the literature. Measurements were taken as an average of duplicates and experiments were repeated at least twice. The percentage (%) value in brackets on the x axis is the survival of mice treated at day 2 of infection with 100 μg of antibody in the VIC study (Saphire et al., 2018).

(E) Association between treatment at day 2 of infection with human mAbs that neutralize $\geq 50\%$ E-S-FLU and survival $p < 0.0001$ (2-tailed Fisher's exact test).

(F) Range of affinity constants for mAbs isolated from vaccinated donors compared to established therapeutic mAbs: 114, 100, 6D6, and c13C6. RBR, receptor binding region; GC, glycan cap; MLD, mucin-like domain; IFL, internal fusion loop. The measurements were repeated at least twice.

See also Tables S3 and S4.



10 non-neutralizing antibodies provided 31% overall survival (range, 10%–50%); two tailed $p < 0.0001$ by Fisher's exact test (Figure 1E). These results confirmed that neutralization detected in our assay was associated with a therapeutic effect in mice, but also emphasized that some neutralizing antibodies fail to protect, and some non-neutralizing antibodies can protect, at least partially.

Diversity of Epitopes Recognized

We defined the epitopes recognized by antibodies with four assays. First, we measured competitive inhibition of binding by antibodies with defined specificities including our own mAb P6 (glycan cap, GC). P6 was designated as specific for the GC by alanine scanning and electron microscopy in the VIC study (Saphire et al., 2018) where P6 = VIC 82, c13C6 (GC or receptor binding region [RBR]), 114 (RBR), KZ52 (base), c2G4 and c4G7 (base), 100 (base), and 6D6 (fusion loop) as guide antibodies (Figure 2A). Second, a sub-group of antibodies were mapped for binding to a yeast surface display antigenic library expressing GP fragments (Figures 2B and S1; Table S2). Third, binding to thermolysin digested GP to mimic cathepsin removal of glycan cap and mucin-like domain (MLD) (Figures 2C, 2D, and S2). Fourth, binding to MDCK-SIAT1 cells transduced to express MLD-deleted GP (amino acids 313–463 deleted) (Figure S3). With this combination of tests, we could distinguish seven clusters of antibody binding sites: three clusters in the glycan cap, one in the RBR, two in the base or fusion loop, and one in the MLD (summarized in Figure 2D).

Antibodies to Glycan Cap

mAbs to the GC could be divided into three overlapping groups. In the first group (exemplified by P6 = VIC 82 and 040 = VIC 91) the antibodies cross-inhibited the binding only of other GC-specific antibodies (Figure 2A). P6 was defined as GC-specific by electron microscopy and alanine scanning (Saphire et al., 2018), and both P6 and 040 were defined by sequencing of a protein fragment consisting of amino acids 228–281 of GP1 expressed in yeast that was bound by these antibodies (Figures 2B and S1; Table S2). The epitopes bound by antibodies to the GC were removed by thermolysin cleavage of GP expressed on MDCK-SIAT1 cells (GPcl) (Figures 2C and S2). In the second group, the antibodies inhibited the binding of both GC-specific

antibodies and RBR-specific antibodies, as exemplified by 66-3-2C (Figure 2A), which suggests they bind to an epitope that overlaps these two regions.

The third group was defined by antibody 66-3-9C that bound to a small conserved peptide within the β 17–18 loop of the glycan cap (amino acids 286–293 GEWAFWET) expressed in yeast (Figure 2B, iii). 66-3-9C recognizes a similar epitope to that bound by the macaque-derived mAb FVM09 (Keck et al., 2015). The disordered loop is juxtaposed to the surface footprint bound by the base antibody KZ52 (Keck et al., 2015), which may explain why KZ52 blocked the binding of biotinylated 66-3-9C (Figure 2A). FVM09 was found to synergize with certain other mAbs to the GC and base for *in vitro* neutralization and protection *in vivo* (Howell et al., 2017). We noted mutually enhanced binding between the base antibodies c2G4 and c4G7 and 66-3-9C (Figure 2A). However, this mutually enhanced binding did not translate to enhanced neutralization by mixtures of these antibodies in our *in vitro* assay (data not shown).

The GC-specific antibodies defined by the competition assay lost binding to thermolysin-treated GP expressed on MDCK-SIAT1 cells (Figures 2C and S2).

Antibodies to the Receptor Binding Region

The RBR is highly conserved in species of *Ebolavirus* and *Marburgvirus* and therefore offers an attractive target for therapeutic antibodies (Murin et al., 2014; Hashiguchi et al., 2015; Flyak et al., 2015; Bornholdt et al., 2016; Corti et al., 2016). We defined mAbs to the RBR by competition for binding to GP with human mAb 114. We showed that 114 bound the GP1 core fragment 102–230 in the yeast expression assay (Figure 2B). mAb 114 competed for binding with a subset of neighboring GC-specific antibodies (Figure 2A) but not with P6 and 040. However, in contrast to the GC-specific antibodies, mAb 114 and similar antibodies retain binding after release of the GC and MLD following exposure of E-SIAT cells to thermolysin digestion as expected (Corti et al., 2016; Misasi et al., 2016) (Figures 2C and S2). Ten mAbs showed this pattern and were placed into the RBR binding group (Figure 2).

Antibodies to the Base or Fusion Loop

These antibodies were defined by competition for binding with the published antibodies KZ52 (base), c2G4 and c4G7 (base), 100 (base), and 6D6 (fusion loop). Many of these antibodies

Figure 2. Identification of Epitopes

(A) Antibody epitopes defined by cross-inhibition for binding. Known antibodies 114, ZMapp (c13C6, c2G4, c4G7), 100, and KZ52 were used as guide mAbs to group other antibodies. Antibodies 66-4-A8 (MLD-dependent mAb) and influenza antibodies were used as non-inhibiting controls. Red designates inhibition of the biotinylated antibody by the competing antibody. Blue designates absence of inhibition in the presence of competing antibody. Inhibition values were calculated as defined in STAR Methods. Results are the average of repeated experiments and 4–8 replicates were included in each measurement.

(B) A selection of mAbs 040 (i), 114 (ii), and 66-3-9C (iii) was screened for binding a yeast display library of fragments of EBOV GP. The fragments recognized are represented on the structure of the KZ52-GP complex PDB: 3CSY.

(C) Binding of mAbs to Ebola GP on transduced MDCK-SIAT1 cells (E-SIAT) after thermolysin digestion, analyzed by flow cytometry. Log of the difference of binding of mAbs to thermolysin-treated E-SIAT and thermolysin-untreated E-SIAT is shown: Bars are color coded by the specificity of the mAbs as defined by the competition binding assays: purple, glycan cap; black, mucin-like domain; green, receptor binding region; orange, base, and gray, undefined. An arbitrary value of 0.2 is used as a cut-off to define mAbs affected by thermolysin digestion, with reference to mAb 114, which is known to be resistant to thermolysin digestion. The measurements were repeated at least twice.

(D) Assignment of neutralizing or protective antibodies to their epitopes based on cross-inhibition assays. (i) Mucin-like domain-dependent. Six mAbs lost binding to the MLD deleted GP. 66-3-9C (specific for the β 17–18 loop) and the base antibody 66-4-C12 also showed reduced binding. (ii) Glycan cap and receptor binding region. P6-like (GC), 114-like (RBR), and others in-between these epitopes. P6-like and 114-like are independent epitopes and do not block each other. Antibodies on the left (P6-like and neighbors) are sensitive to thermolysin cleavage. Antibodies on the right (114-like) are resistant to thermolysin cleavage or have enhanced binding after cleavage. (iii) Antibodies to base are blocked by defined base antibodies and are resistant to thermolysin digestion.

See also Figures S1, S2, and S3 and Table S2.

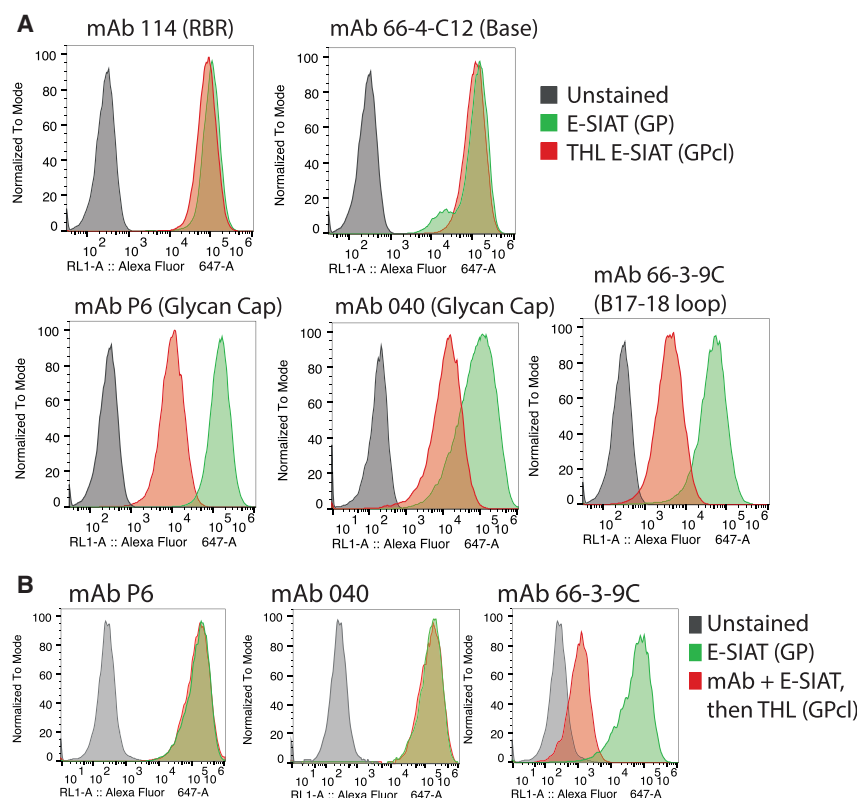


Figure 3. Effect of Glycan Cap-Specific Antibodies on Cleavage by Thermolysin (GPcl)

(A) Binding by glycan cap antibodies is sensitive to thermolysin cleavage, but binding by antibodies to the RBR and base is not. GC, glycan cap; RBR, receptor binding region; THL, thermolysin; E-SIAT, MDCK-SIAT1 cells expressing Ebola virus glycoprotein.

(B) Binding by some glycan cap antibodies survives treatment by thermolysin if present during digestion. Experiments were reproduced at least three times. See also Figure S2.

This is reflected in the loss of binding by antibodies to the glycan cap and MLD to E-SIAT cells after exposure to thermolysin (Figures 2, 3, and S2). We noticed that some antibodies to the glycan cap, if bound before exposure of E-SIAT cells to thermolysin treatment, remained bound after thermolysin treatment (Figures 3B and S2C).

Figure 3A shows binding of selected GC-, RBR-, and base-specific antibodies after cleavage by thermolysin. The three antibodies to the glycan cap (P6, 040, and 66-3-9C) lose binding after thermolysin treatment, whereas the epitopes bound by RBR (114)- and base (66-4-C12)-specific antibodies were not affected (Figures 3A and S2). We confirmed this result for seven additional GC-specific antibodies (Figure S2). Thermolysin digestion achieved complete removal of these epitopes as shown by (1) the reduction of binding by these antibodies to the level of a negative control specific for influenza (Figure S2), (2) the appearance of the epitope recognized by MR78 that binds to EBOV GP only after removal of the glycan cap (Flyak et al., 2015; Bornholdt et al., 2016; Hashiguchi et al., 2015), and (3) loss of detection in western blots of the GP1 fragment bound by P6 (Figure S2D).

We next noted the effect of allowing the GC-specific antibodies to bind, followed by treatment with thermolysin. We found that the mAbs P6 and 040 remained bound despite thermolysin treatment (Figure 3B). This effect was confirmed (Figure S2) for five additional neutralizing antibodies to the GC (66-3-7C, 66-3-2C, 141, 66-3-4A, and 125). The effect was specific to glycan cap-specific antibodies and not seen for antibody 66-3-9C specific for the β 17-18 loop (GEWAFWET) (Figure 3B).

In these experiments, the E-SIAT cells were first trypsinized to detach them from plastic before exposure to thermolysin. We repeated the experiment without the use of trypsin, where the cells were exposed only to thermolysin in plastic plates. Thermolysin treatment resulted in the loss of binding sites for the nine GC-specific antibodies tested. Evidence for cleavage in these conditions was provided by the appearance of the epitope in RBR bound by MR78 that only binds to EBOV GP after removal of the glycan cap (Figure S2B). When E-SIAT cells

cross-inhibited each other, but sub-groups were discernible. For instance, biotinylated 6541 and 66-4-C12 were both inhibited by the characterized base antibodies KZ52 and 100, but 6541 and 66-4-C12 failed to inhibit each other, suggesting that they bound to non-overlapping sites in the base region (Figures 2A and 2D). Antibodies 6541, 66-4-C12, and 66-6-3 competed for binding with the fusion loop-specific murine mAb 6D6, which suggested their binding footprints may overlap with the fusion peptide. Binding of base region-specific antibodies to thermolysin-treated cells was typically either unaffected or enhanced (Figures 2C and S2).

Mucin-like Domain-Dependent Antibodies

The binding of 6/82 antibodies to MDCK-SIAT1 cells expressing GP lacking the MLD (amino acids 313–463) was reduced by comparison with cells expressing full-length GP (Figure S3). Control antibodies to GP1 head (c13C6) and base (KZ52 and c4G7) bound the MLD deleted and full-length GP equally. None of the six MLD-dependent antibodies were neutralizing. We found that the antibodies 66-3-9C (specific for the β 17-18 loop sequence [GEWAFWET]) also lost binding to the MLD-deleted GP, and the binding of one antibody to the base, 66-4-C12, was reduced (although was not affected by thermolysin cleavage).

Antibodies to the Glycan Cap and Thermolysin Cleavage

Treatment with thermolysin mimics the effect of cathepsin and results in removal of the GC and MLD (Chandran et al., 2005; Schornberg et al., 2006; Côté et al., 2011; Miller et al., 2012).

were treated with thermolysin in the presence of GC-specific antibodies, these antibodies retained their binding, with the exception of 66-3-9C to the β 17-18 loop (Figure S2C).

A western blot in Figure S2D shows that immunoprecipitation by the P6 (GC) antibody of the bands representing GP1 detected after blotting by a mAb to the sequence GEWAFWET (286–293) is lost after thermolysin treatment. This indicates the completeness of digestion in these conditions and correlates with the loss of binding of P6 and other GC antibodies in the indirect immunofluorescence assays in Figure S2B.

These results suggested that the P6, 040, and other neutralizing GC-specific antibodies may have either inhibited cleavage of GP by thermolysin or stabilized the glycan cap in the bound state despite cleavage. A related observation has been made recently with the GC-specific mAb EBOV-442 (Gilchuk et al., 2018).

Cross-Reactivity of the Antibodies

SUDV Gulu and MARV GP proteins were expressed by the booster MVA vaccine, which may have stimulated cross-reactive clones. We looked for cross-reactivity of our collection of antibodies to glycoproteins of EBOV Mayinga 1976 (AF086833) and to other Ebola virus species—BDBV (NC_014373.1) and SUDV Gulu (NC_006432.1). Although there is only 55% and 65% sequence homology to SUDV and BDBV GP protein sequences (Figure S4), it is notable that of 82 antibodies selected for binding to EBOV glycoprotein, 20 were cross-reactive in binding to some level on the glycoproteins of Bundibugyo and Sudan species expressed in MDCK-SIAT1 cell (Figures 4A and 4B). Of the subset of neutralizing or protective antibodies (Figure 6F), we identified examples that were cross-reactive in binding to BDBV and SUDV GP-specific for the base (66-4-C12, 6651, 6541), glycan cap (040), the β 17-18 loop amino acids 286–293 (66-3-9C), and the RBR (6662) (Figure 4C). It is evident that pan-Ebolavirus antibodies to the fusion loop can also be isolated (Zhao et al., 2017; Furuyama et al., 2016; Wec et al., 2017), however, we have not delineated this epitope in our study.

Diversity in Gene Usage and Affinity Maturation

Twenty-three V_H genes encoded the 82 antibodies from 11 donors, making the V_H gene use very diverse within the collection and within the individual donors (Figure 5A). Almost equal numbers of antibodies possessed the Kappa ($n = 39$) or Lambda ($n = 43$) light chain. V_H 3-15 was the most commonly used germ-line gene and it encoded 20 antibodies in 10 donors (Figure 5A; Table S1).

Most of the antibody sequences have high identity to their germline genes with an average of five somatic mutations giving rise to amino acid changes (Figures 5B and 5C). This is expected for antibodies that have been recently stimulated with minimal engagement in the germinal center reaction, as previously reported in the response to vaccination or infection with H7 hemagglutinin (Thornburg et al., 2016; Huang et al., 2019). The number of somatic mutations in these Ebola antibodies is lower than that of antibodies to seasonal influenza derived from individuals that are likely to have been repeatedly exposed (Huang et al., 2015; Pappas et al., 2014; Wrammert et al., 2011).

V_H 3-15 and V_λ 1-40 Antibodies to the Receptor Binding Region

Overall, there was no particular favored V_H gene identified among neutralizing antibodies, which can be seen in the response to some viruses such as pdmH1N1 influenza (Jackson et al., 2014) and dengue (Parameswaran et al., 2013) for which signature V_H genes were identified. Interestingly, however, out of a total of 39 mAbs for which we have identified the epitopes (6 to MLD, 14 to glycan cap, 10 to RBR, and 9 to base), all ten mAbs that competed with the RBR-specific antibody 114 (V_H 3-13/ V_λ 1-27) are encoded by V_H 3-15 and V_λ 1-40 genes and none by other V_H genes. These ten V_H 3-15 RBR mAbs come from six donors (Figures 2D and 5A). One out of ten, 6662, cross-reacted in binding on EBOV, SUDV, and BDBV GPs (Figures 4 and 6G).

Binding Kinetics Compared to Established Therapeutic Antibodies

In view of the relative temporal immaturity of our collection of antibodies, we measured the binding kinetics and calculated the binding affinity constants (Figure 1F; Table S3) for a selection of antibodies and compared these to established therapeutic antibodies: 114 (RBR) and 100 (base), 6D6 (fusion loop), and c13C6 (RBR or GP1 core). The kinetics of the antibodies were similar in range to the control antibodies (Table S4). Our measurements for 114, 100, and c13C6 gave very similar association rates but somewhat faster dissociation rates (for 114 and 100) to those previously reported (Misasi et al., 2016). This may be related to the use of MLD-deleted molecules compared to complete GP in our measurements.

Selection of Antibody Cocktails for Protection in Guinea Pigs

We selected seven antibodies (Figures 6A and 6F) to test for therapeutic protection in guinea pigs against the EBOV Mayinga virus as described (Dowall et al., 2016). We formed three antibody cocktails from these antibodies—two EBOV-specific cocktails and one containing antibodies that cross-reacted in binding to BDBV and SUDV GPs. The selection of the antibodies was based on four characteristics: (1) neutralization in our E-S-FLU assay, because this correlated with protection of mice in the VIC study, (2) binding independently to non-overlapping epitopes in GC, RBR, and base, because we wished to reduce the likelihood of selecting antibody resistant variants during treatment *in vivo* (Kugelman et al., 2015), (3) protection in mice where this information was available from the VIC study, and (4) cross-reactivity for Bundibugyo and Sudan GPs (Figures 6F and 6G) for the group 3 cocktail, because the long term goal is to find a single treatment that will work for these three species that cause the majority of infections in humans.

The three cocktails were tested at a dose of 10 mg/Kg of each antibody (groups 1–3). This dose was selected partly on our experience with protective antibodies in influenza infection, and also because the affinities of the antibodies, and binding assays *in vitro*, suggested that 10 mg/Kg ($\sim 10 \mu\text{g/mL}$) should be close to saturation. The first cocktail, which we expected to be the most potent from the evidence available, was also tested at 5 mg/Kg total (equivalent to 1.67 mg/Kg of each

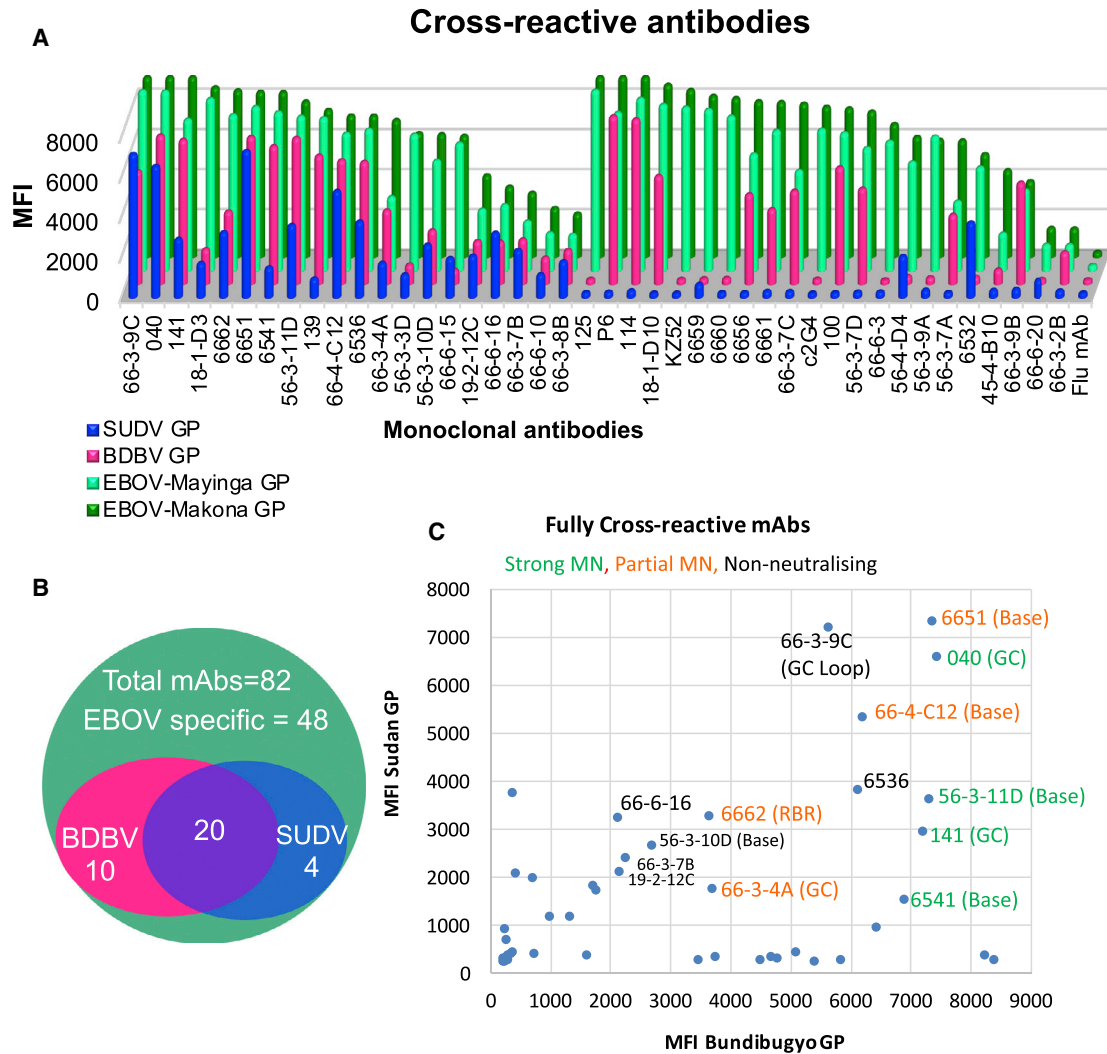


Figure 4. Twenty out of 82 mAbs Are Cross-Reactive to Both Sudan and Bundibugyo GPs

(A) Monoclonal antibodies were compared by indirect immunofluorescence for binding to MDCK-SIAT1 cells expressing GPs from different *Ebolavirus* species. MFI, mean binding fluorescence intensity.

(B) Venn diagram showing the frequencies of cross-reactive antibodies. Twenty of 82 showed some level of cross-reactivity between the three species of GP.

(C) A selection of Ebola virus reactive antibodies was compared for binding to BDBV and SUDV GPs. Measurements of binding were repeated at least twice.

antibody) (group 4) for comparison to ZMapp given at the same dose. This dose was not expected to be 100% curative and should furnish an opportunity to test for equivalence to ZMapp. The first and second cocktails differed in the RBR mAb, where 6662 (that was highly protective in the murine challenge) replaced 6660. The third cocktail (group 3) was composed of four mAbs that cross-react in binding to EBOV, SUDV, and BDBV glycoproteins. In addition to mAbs specific for epitopes in GC, RBR, and base, it included 66-3-9C specific for the β 17-18 loop because of its similarity to FMV09 (Howell et al., 2017) that provided a synergistic therapeutic effect. Controls were ZMapp at a dose of 5 mg/Kg (kindly supplied by Larry Zeitlin) and PBS.

When tested as cocktails in the neutralization assay, groups 1 and 2 were EBOV-specific, and group 3 showed additional

partial neutralization of S-FLU coated in BDBV and SUDV GPs (Figure 6B-6E). The control antibody 6D6 strongly neutralized S-FLU coated in GPs from all the *Ebolavirus* species. Binding of individual antibodies in group 3 to EBOV, BDBV, and SUDV GPs is shown in Figure 6G. Binding of mAb 6541 to SUDV GP showed prozone effect.

Therapeutic Protection of Guinea Pigs by Antibody Cocktails

Guinea pigs were challenged with 10^3 TCID₅₀ of guinea pig adapted Ebola virus in 200 μ L volume subcutaneously and treated on day 3 with the antibody mixtures by intraperitoneal injection in 2 mL volume, at the Porton Down high containment facility. Animals were monitored for temperature and clinical signs and were culled if they reached 10% weight loss and clinical

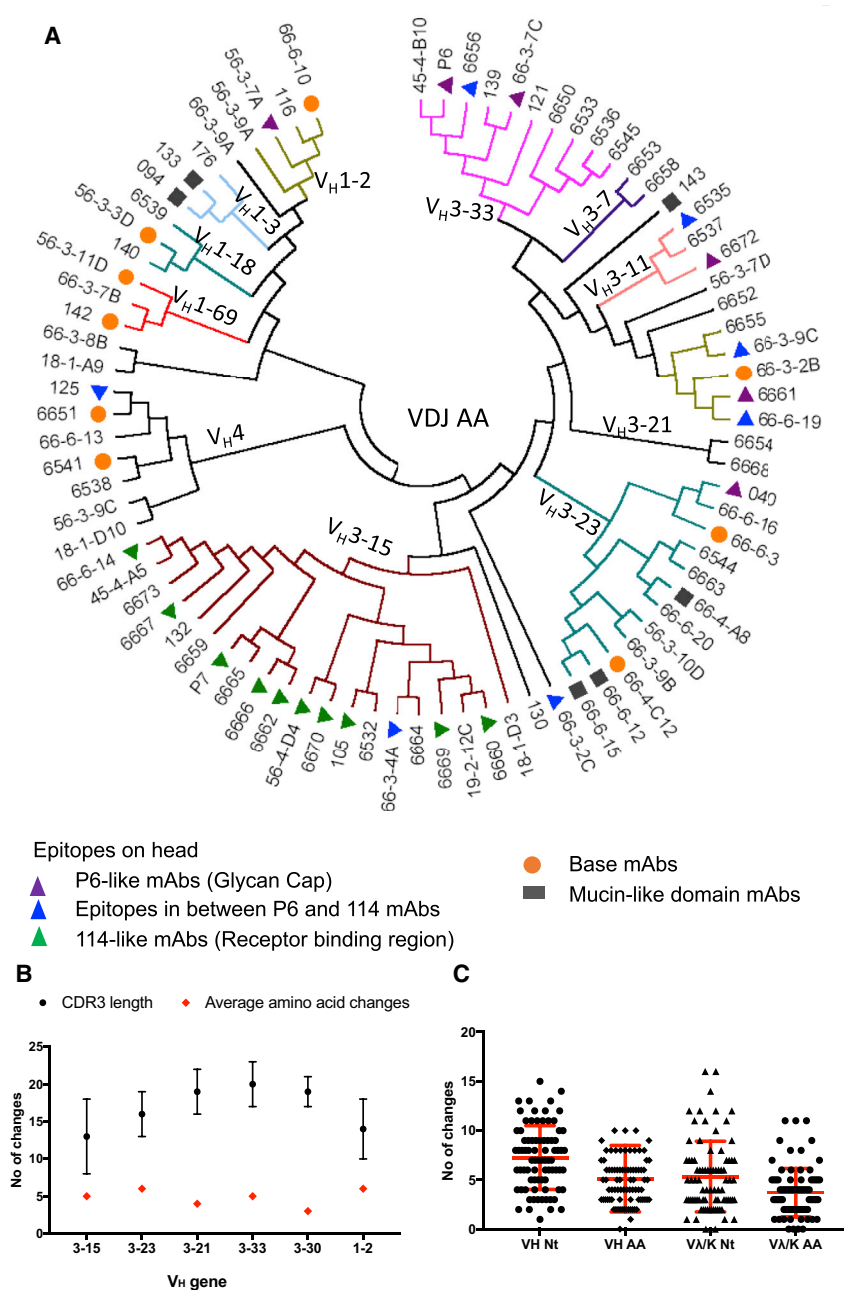


Figure 5. Gene Use and Characteristics of V_H Genes

(A) Phylogeny of the antibodies based on VDJ amino acid sequences. More than 23 V_H genes have been used altogether. V_H3-15 was the most used gene and all ten antibodies that recognize the 114-like epitope in the RBR were encoded by this V_H gene. The tree was drawn using MEGA v7 software and alignment was done using Neighbor-joining tree settings.

(B) CDR3 length (mean ± SD) and average frequency of amino acid substitutions in the largest sets of V_H genes.

(C) Number of amino acid (AA) and total nucleotide (nt) changes in V_H and V_κ genes of the eighty-two EBOV GP-specific antibodies isolated from vaccinated donors shown in Table S1.

only 1 out of 6 animals. In group 3, treatment with the cross-reactive cocktail comprised of four independently binding antibodies (040 + 66-3-9C + 6662 + 6541) resulted in 100% survival without weight loss or clinical signs (Figures 7A and 7B).

Animals that met humane endpoints all had high levels of detectable EBOV RNA in blood, liver, and spleen. Animals that survived until the end of the study (21 days post-challenge) had no detectable viral RNA (Figure S5). These results were confirmed by *in situ* hybridization analysis of samples and the absence of Ebola virus-induced lesions and histological changes in surviving animals compared to those in non-survivors (Supplemental Pathology Report).

DISCUSSION

The antibody response to EBOV GP in vaccinated donors was very diverse both in terms of the range of the >23 V_H genes used to generate the 82 antibodies and the diversity of epitopes detected. Antibodies to the glycan cap were most abundant (Flyak et al., 2016), but antibodies to

score ≥3 or weight loss of ≥20% similar to a previously described study (Dowall et al., 2016).

The group 1 cocktail (125 + 6660 + 66-6-3) resulted in 4 out of 6 guinea pigs surviving (Figure 7). The same cocktail given at lower dose (1.67 mg/Kg each) in group 4 resulted in 3 out of 6 animals surviving, which was the same as ZMapp at the same dose. In previous studies, a higher dose of ZMapp (5 mg/animal) resulted in complete survival in this model when given by the intravenous route (Dowall et al., 2016). Survival in group 2 (125 + 6662 + 66-6-3), which differed from group 1 only in replacement of the RBR-specific mAb 6660 with 6662, was

the RBR, base, and mucin-like domain were also common. The diversity in the epitopes recognized in the response of vaccinees to EBOV GP contrasts with the response to seasonal influenza hemagglutinin, where in some individuals after repeated exposures over years, the response can be focused onto a localized patch of the HA molecular surface (Huang et al., 2015; Linderman et al., 2014).

The range of specificities, cross-reactivity with other *Ebolavirus* species, and binding kinetics of a subset of the antibodies from vaccinees, despite being relatively immature with few somatic mutations, were comparable to antibodies isolated from

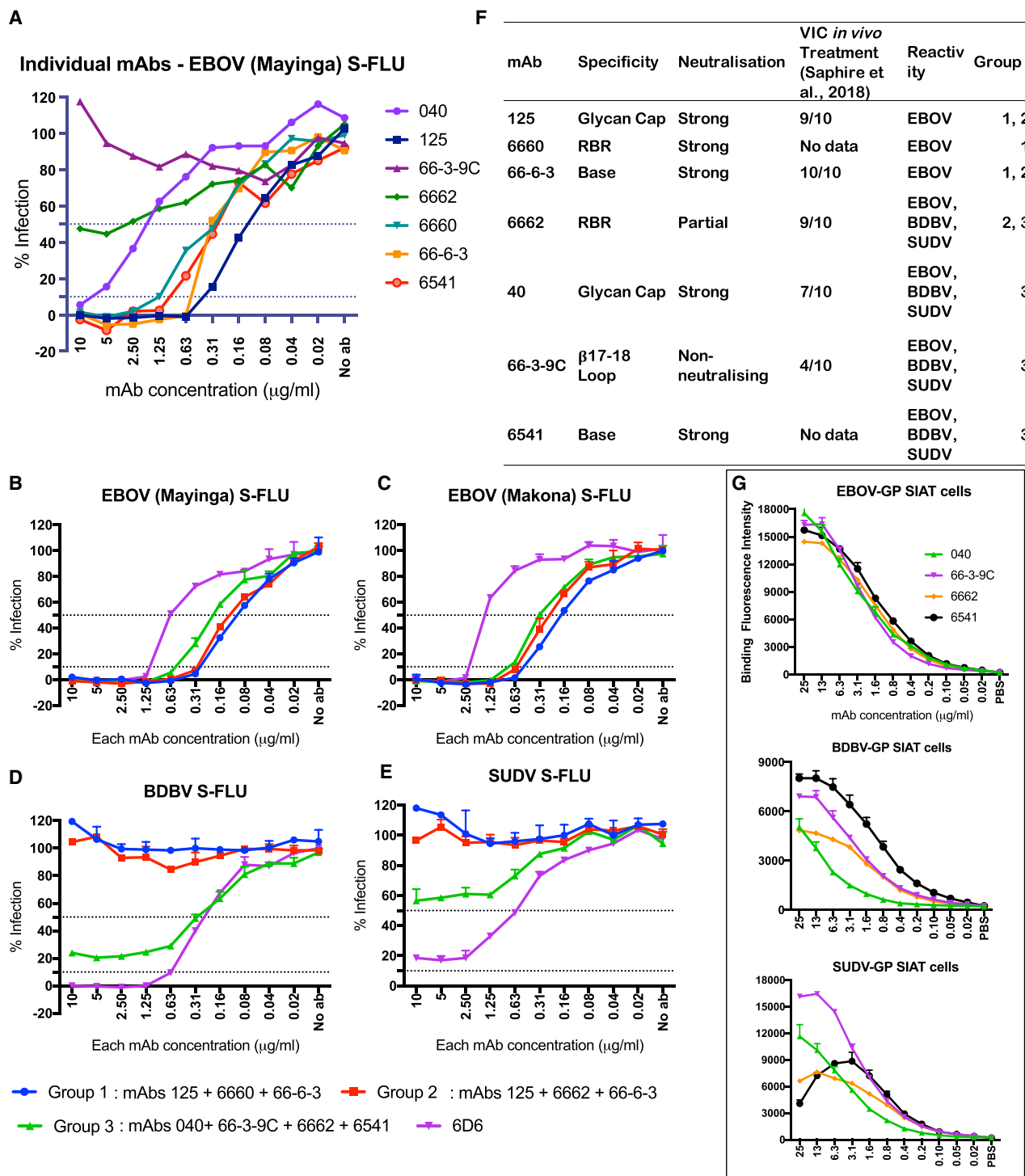


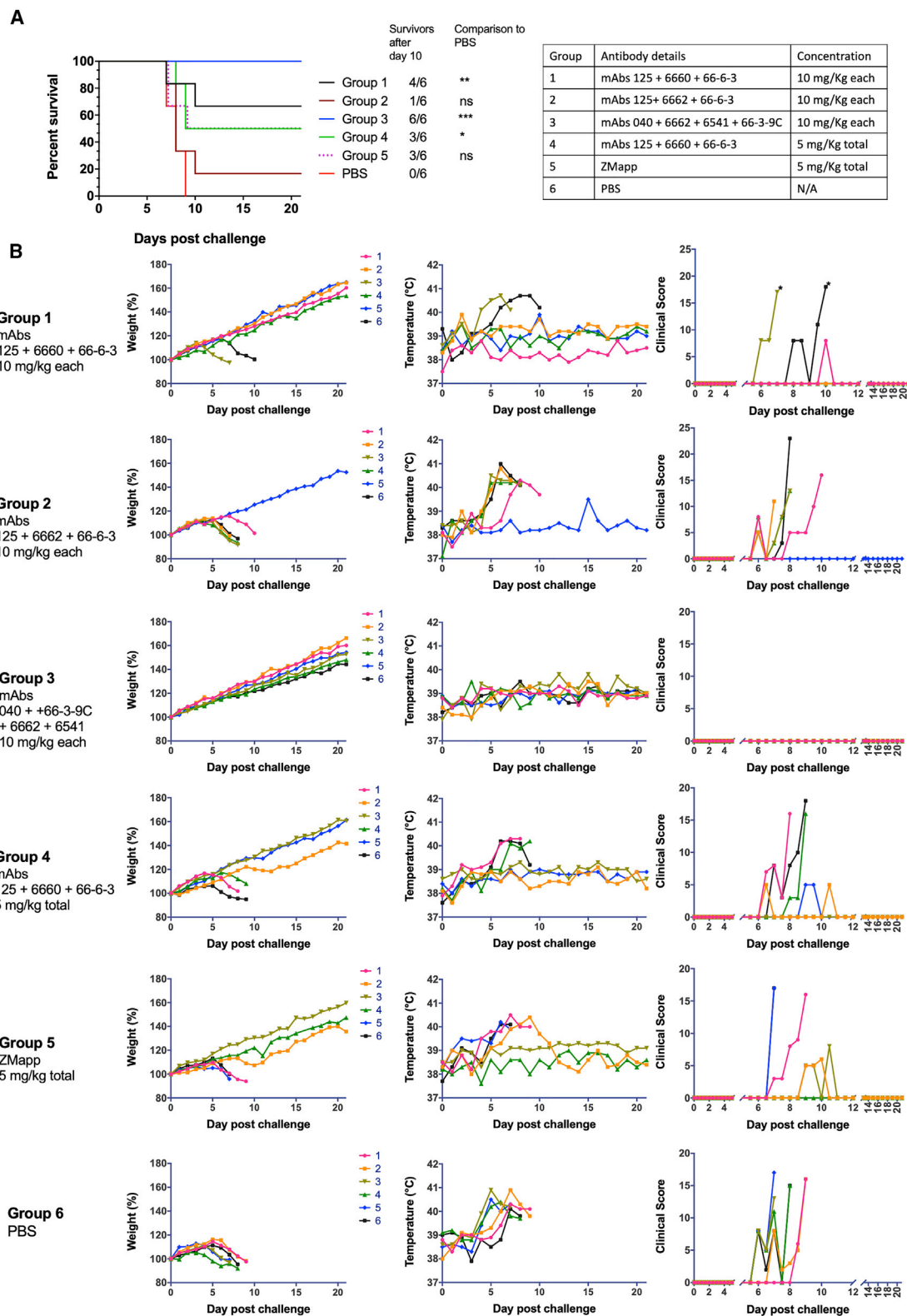
Figure 6. Selection of Antibody Cocktails

(A) Neutralization of pseudotyped virus by seven mAbs selected for inclusion in three antibody cocktails. Antibodies were selected on four criteria: (1) neutralization, (2) ability to protect mice from EBOV infection (as part of the VIC collaboration), (3) mutually exclusive binding to separate epitopes on GP, and (4) cross-reactivity with BDBV and SUDV GPs.

(B–E) Neutralization of pseudotyped viruses by the selected antibody cocktails: EBOV Mayinga (B), EBOV Makona (C), BDBV (D), and SUDV (E). Each data point represents an average of duplicates \pm SD. Experiments were repeated at least three times.

(F) Characteristics of antibodies selected for inclusion in the cocktails for the guinea pig trial.

(G) Binding titrations of cross-reactive group 3 mAbs on EBOV, BDBV, and SUDV GPs expressed on MDCK-SIAT1 cells.



(legend on next page)

convalescent humans, or multiply immunized mice or macaques (Saphire and Aman, 2016; Zhao et al., 2017; Pascal et al., 2018; Misasi et al., 2016). A similar phenomenon was seen in the human immune response to avian H7 influenza hemagglutinin after primary natural infection or vaccination, where a subset of antibodies close to germline in sequence was powerfully neutralizing *in vitro* and protective *in vivo* (Thornburg et al., 2016; Huang et al., 2019). Earlier work had also emphasised that high-affinity protective antibodies appeared early in the murine response to VSV (reviewed by Zinkernagel, 2002).

We developed an assay to screen the antibodies for neutralization. This uses a single-cycle influenza core with the hemagglutinin coding sequence replaced with eGFP for detection of infected cells and coated in the EBOV GP by pseudotyping (Xiao et al., 2018). As this virus can replicate only for a single cycle, and contains no genetic information from Ebola, it can be handled in more convenient containment conditions than Ebola virus. In collaboration with the VIC, we established that our neutralization assay correlated reasonably with therapeutic activity in mice (Saphire et al., 2018). We used the assay to narrow the choice of antibodies to combine in therapeutic cocktails.

The mechanisms by which antibodies protect against Ebola virus *in vivo* are not fully understood. Antibodies to epitopes in the glycan cap, RBR, and base or fusion loop can all neutralize *in vitro* and protect *in vivo* (Saphire et al., 2018). Suggested mechanisms include blockade of NPC1 binding, prevention of cathepsin cleavage, interference with fusion, and Fc-dependent interactions with host cells (reviewed in Saphire et al., 2018; Gunn et al., 2018). Certain base binding antibodies have been shown to prevent cathepsin cleavage (Shedlock et al., 2010; Misasi et al., 2016; Wec et al., 2017), and the epitopes bound by base antibodies are usually retained after cleavage by thermolysin (as a cathepsin surrogate) (Figure 2C). Antibodies that bind the glycan cap can neutralize *in vitro* and provide protection *in vivo*, but it is not clear how this can occur if the epitope is removed by cathepsin cleavage before GPcl binds to NPC1. We found that neutralizing and protective antibodies to the glycan cap including P6 (VIC 82) and 040 (VIC 91), had the property that once bound to GP expressed on the membrane of transduced cells, they remained bound after exposure to thermolysin. This effect was specific, because binding of the antibody 66-3-9C that binds the β 17-18 loop on the glycan cap did not survive exposure to thermolysin treatment (Figure 3). If the GP was treated with thermolysin first, all nine GC-specific antibodies showed greatly reduced binding (Figures 2C and S2). A similar observation was made recently for the GC-specific mAb EBOV-442 (Gilchuk et al., 2018). Although not definitive, these results suggest that some antibodies bound to the glycan cap may neutralize either through interference with cathepsin cleavage or by stabilizing the glycan cap in the bound state despite thermolysin cleavage.

Due to the high mutation frequency of Ebola virus (Carroll et al., 2015; Alfson et al., 2015), mAbs, even when given in combination, can select escape mutants during treatment of non-human primates (Kugelman et al., 2015). Therefore, we aimed to find sets of neutralizing antibodies that bound independently to sites in the glycan cap, receptor binding region, and base of GP, to limit the selection of resistant mutants and maximize the likelihood of combining several mechanisms of protection. From 82 antibodies isolated from 11 vaccinated donors, we formed three antibody cocktails. Groups 1 and 2 were selected for their apparent strength of neutralization *in vitro* and protection in the mouse infection assay performed within the VIC study (Saphire et al., 2018). Neither of these cocktails provided complete protection, and therefore it is possible they selected resistant escape viruses. We intend to sequence the viral RNA from the tissues of these animals in a follow up study.

Group 3 was selected first on the level of cross-reactivity in binding between the GPs from the three Ebola virus species Zaire, Bundibugyo, and Sudan and second on their neutralization and mouse protection. It is notable that cross-reactive antibodies can be found that bind glycan cap, RBR, and base or fusion loop. Treatment of guinea pigs at day 3 of infection with the cross-reactive cocktail of four antibodies that included 040 to glycan cap, 6662 to the RBR, 6541 to the base, and 66-3-9C to the β 17-18 loop, resulted in 100% protection from a lethal EBOV infection, without weight loss or clinical signs. Viral RNA was not detected in the tissues of these animals at post mortem on day 21 post infection, which implies that selection of resistant virus variants did not occur. We plan to test the group 3 cocktail for efficacy in the ferret model against EBOV, SUDV, and BDBV virus species (Kroeker et al., 2017; Kozak et al., 2016).

The effectiveness of this combination could not have been predicted from the *in vitro* neutralization or murine protection results with individual antibodies. The β 17-18 Loop-specific antibody 66-3-9C is closely related to the FVM09 antibody (Keck et al., 2015; Howell et al., 2017) isolated from cynomolgus macaques. FVM09 is specific for the conserved exposed loop between beta strands 17 and 18 with the sequence GEWAFWET and by itself is not neutralizing *in vitro* and was only weakly protective *in vivo*. However, FVM09 in mixtures enhanced the binding and neutralization by base antibody 2G4, and the GC-specific antibody m8C4 (Holtsberg et al., 2015; Howell et al., 2017). *In vivo* FVM09 enhanced protection by the GC-specific antibody m8C4 (Howell et al., 2017) and a fusion loop-binding antibody FVM02p (Keck et al., 2015). A structural analysis of the synergistic effect of FVM09 with a base-binding antibody ADI-15946 suggests that FVM09 peels the GEWAFWET loop away from the binding site for ADI-15946 and thus enhances its capacity to bind and neutralize (West et al., 2018). 66-3-9C is specific for the same sequence as FVM09 (Figure 2B), does not neutralize *in vitro*, and provides only modest protection *in vivo* in the mouse (4 out of 10 survivors). We also saw reciprocal

Figure 7. Therapy of Guinea Pigs Infected with Ebola VIRUS with Mixtures of Antibodies

(A) Survival curves for the guinea pigs (n = 6) treated with the antibody cocktails on day 3 of infection. Kaplan-Meier survival curves were analyzed with the log-rank (Mantel-Cox) test.

(B) Body weight (column 1), body temperature (column 2), and clinical scores (column 3).

See also Figure S5.

enhanced binding between 66-3-9C and the base antibodies c2G4 and c4G7, but this did not extend to enhanced neutralization in our assay. However, the profound therapeutic effect of the mixture of antibodies containing 66-3-9C suggests it may have had a synergistic effect *in vivo*. Antibodies to the conserved loop between the β 17-18 strands may be a generally useful addition to therapeutic mixtures of antibodies.

In summary, we have shown that an experimental Ebola virus vaccine trial offers a valuable opportunity for the isolation of potentially therapeutic human mAbs. We suggest that isolation of mAbs should accompany all experimental vaccine trials for emerging pathogens, for which specific therapies are lacking.

STAR★METHODS

Detailed methods are provided in the online version of this paper and include the following:

- **KEY RESOURCES TABLE**
- **CONTACT FOR REAGENT AND RESOURCE SHARING**
- **EXPERIMENTAL MODEL AND SUBJECT DETAILS**
 - Ethics Statement
 - Human PBMC
 - Guinea Pigs challenge studies
 - Cell Lines
 - MDCK-SIAT cells expressing Ebola GP and MLD-deleted GP
 - Viruses
- **METHOD DETAILS**
 - Isolation of mAbs from plasmablasts
 - Isolation of mAbs from memory B cells
 - Immunofluorescence Binding Assays
 - Expression and Purification of Antibody
 - Expression and purification of soluble glycoproteins
 - Virus Neutralisation Assays
 - Epitope Mapping using Competitive Binding Assays
 - Epitope Mapping using Yeast Peptide-Display Assays
 - Binding Kinetics using Surface Plasmon Resonance (SPR)
 - Thermolysin Digestion
 - PCR of guinea pig tissues
 - Histological analysis of guinea pig samples
 - Gene family usage of IgG genes
- **QUANTIFICATION AND STATISTICAL ANALYSIS**
- **DATA AND SOFTWARE AVAILABILITY**

SUPPLEMENTAL INFORMATION

Supplemental Information can be found online at <https://doi.org/10.1016/j.celrep.2019.03.020>.

ACKNOWLEDGMENTS

We are grateful to Antonio Lanzavecchia, Davide Corti, and Larry Zeitlin for providing antibodies 114, 100, and ZMapp cocktail. We thank Erica Saphire for inviting us to take part in the VIC study, and helpful comments on the manuscript. We thank Vincenzo Cerundolo for the departmental support. We thank Amy Duckett and Carly Banner for arranging contracts; Jack Tan, Julie Furze, Drew Worth, Daniel Alanine, Teresa Lambe, Matthew Edmans, and Vincent Pavot for assistance with mAb isolation and/or analysis, the EBL01 clinical trial

study volunteers, as well as Adrian Hill and the clinical trials team at the CCVTM, University of Oxford for access to EBL01 trial samples. We also thank Craig Waugh and Paul Sopp at WIMM FACS Facility. We thank Tom Bowden (STRUBI, Oxford) for the purified Ebola glycoprotein. These studies were funded by a UK Medical Research Council grant to the MRC Human Immunology Unit (MC_PC_15002), the Wellcome Trust (204826/Z/16/Z), and the Townsend-Jeantet Prize Charitable Trust (charity number 1011770). P.R. was funded by the RDM Prize Studentship and the Clarendon Fund in conjunction with the Keble College de Breyne scholarship. S.J.D. is a Jenner Investigator, a Lister Institute Research Prize Fellow, and a Wellcome Trust Senior Fellow (106917/Z/15/Z). Views are those of the authors and do not necessarily reflect those of the funding bodies or employing institutes.

AUTHOR CONTRIBUTIONS

Conceptualization, A.R.T., S.J.D., D.J.L., A.P., G.B., and P.R.; Methodology, P.R., A.R.T., S.C.E., D.J.L., T.B., S.D., E.R., S.F.-W., and J.G.; Investigation, P.R., A.R.T., S.C.E., D.J.L., T.B., V.O.D., S.R.M., L.S., E.B., S.C.M., C.J.C., T.R., S.D., E.R., S.F.-W., J.G., F.R.D., and K.-Y.A.H.; Resources, J.X., J.J., G.M.L., F.R.D., and A.T.; Writing – Original Draft, P.R. and A.R.T.; Writing – Review & Editing, P.R., A.T., S.J.D., S.D., and S.C.E.; Supervision, A.R.T., S.J.D., D.J.L., A.P., D.M., M.C., and X.-N.X.

DECLARATION OF INTERESTS

Authors are named inventors on a patent application relating to Ebola virus mAbs. S.J.D. is a named inventor on patent applications relating to adenoviral vaccines and immunization regimens.

Received: October 11, 2018

Revised: December 10, 2018

Accepted: March 5, 2019

Published: April 2, 2019

REFERENCES

- Alfonso, K.J., Worwa, G., Carrion, R., Jr., and Griffiths, A. (2015). Determination and Therapeutic Exploitation of Ebola Virus Spontaneous Mutation Frequency. *J. Virol.* 90, 2345–2355.
- Bornholdt, Z.A., Turner, H.L., Murin, C.D., Li, W., Sok, D., Souders, C.A., Piper, A.E., Goff, A., Shamblin, J.D., Wollen, S.E., et al. (2016). Isolation of potent neutralizing antibodies from a survivor of the 2014 Ebola virus outbreak. *Science* 351, 1078–1083.
- Carroll, M.W., Matthews, D.A., Hiscox, J.A., Elmore, M.J., Pollakis, G., Rambaut, A., Hewson, R., García-Dorival, I., Bore, J.A., Koundouno, R., et al. (2015). Temporal and spatial analysis of the 2014–2015 Ebola virus outbreak in West Africa. *Nature* 524, 97–101.
- Chandran, K., Sullivan, N.J., Felbor, U., Whelan, S.P., and Cunningham, J.M. (2005). Endosomal proteolysis of the Ebola virus glycoprotein is necessary for infection. *Science* 308, 1643–1645.
- Clargo, A.M., Hudson, A.R., Ndlovu, W., Wootton, R.J., Cremin, L.A., O'Dowd, V.L., Nowosad, C.R., Starkie, D.O., Shaw, S.P., Compson, J.E., et al. (2014). The rapid generation of recombinant functional monoclonal antibodies from individual, antigen-specific bone marrow-derived plasma cells isolated using a novel fluorescence-based method. *mAbs* 6, 143–159.
- Corti, D., Misasi, J., Mulangu, S., Stanley, D.A., Kanekiyo, M., Wollen, S., Ploquin, A., Doria-Rose, N.A., Staupe, R.P., Bailey, M., et al. (2016). Protective monotherapy against lethal Ebola virus infection by a potentially neutralizing antibody. *Science* 351, 1339–1342.
- Côté, M., Misasi, J., Ren, T., Bruchez, A., Lee, K., Filone, C.M., Hensley, L., Li, Q., Ory, D., Chandran, K., and Cunningham, J. (2011). Small molecule inhibitors reveal Niemann-Pick C1 is essential for Ebola virus infection. *Nature* 477, 344–348.
- Davey, R.T., Jr., Dodd, L., Proschan, M.A., Neaton, J., Neuhaus Nordwall, J., Koopmeiners, J.S., Beigel, J., Tierney, J., Lane, H.C., Fauci, A.S., et al.;

- PREVAIL II Writing Group; Multi-National PREVAIL II Study Team (2016). A Randomized, Controlled Trial of ZMapp for Ebola Virus Infection. *N. Engl. J. Med.* 375, 1448–1456.
- Demaision, C., Parsley, K., Brouns, G., Scherr, M., Battmer, K., Kinnon, C., Grez, M., and Thrasher, A.J. (2002). High-level transduction and gene expression in hematopoietic repopulating cells using a human immunodeficiency [correction of immunodeficiency] virus type 1-based lentiviral vector containing an internal spleen focus forming virus promoter. *Hum. Gene Ther.* 13, 803–813.
- Dowall, S.D., Matthews, D.A., Garcia-Dorival, I., Taylor, I., Kenny, J., Hertz-Fowler, C., Hall, N., Corbin-Lickfett, K., Empig, C., Schlunegger, K., et al. (2014). Elucidating variations in the nucleotide sequence of Ebola virus associated with increasing pathogenicity. *Genome Biol.* 15, 540.
- Dowall, S.D., Callan, J., Zeltina, A., Al-Abdulla, I., Strecker, T., Fehling, S.K., Krähling, V., Bosworth, A., Rayner, E., Taylor, I., et al. (2016). Development of a Cost-effective Ovine Polyclonal Antibody-Based Product, EBOTAb, to Treat Ebola Virus Infection. *J. Infect. Dis.* 213, 1124–1133.
- Eisen, H.N., and Chakraborty, A.K. (2013). Immunopaleontology reveals how affinity enhancement is achieved during affinity maturation of antibodies to influenza virus. *Proc. Natl. Acad. Sci. USA* 110, 7–8.
- Ewer, K., Rampling, T., Venkatraman, N., Bowyer, G., Wright, D., Lambe, T., Imoukhuede, E.B., Payne, R., Fehling, S.K., Strecker, T., et al. (2016). A Monovalent Chimpanzee Adenovirus Ebola Vaccine Boosted with MVA. *N. Engl. J. Med.* 374, 1635–1646.
- Flyak, A.I., Illykh, P.A., Murin, C.D., Garron, T., Shen, X., Fusco, M.L., Hashiguchi, T., Bornholdt, Z.A., Slaughter, J.C., Sapparapu, G., et al. (2015). Mechanism of human antibody-mediated neutralization of Marburg virus. *Cell* 160, 893–903.
- Flyak, A.I., Shen, X., Murin, C.D., Turner, H.L., David, J.A., Fusco, M.L., Lampley, R., Kose, N., Illykh, P.A., Kuzmina, N., et al. (2016). Cross-Reactive and Potent Neutralizing Antibody Responses in Human Survivors of Natural Ebola-virus Infection. *Cell* 164, 392–405.
- Flyak, A.I., Kuzmina, N., Murin, C.D., Bryan, C., Davidson, E., Gilchuk, P., Gulka, C.P., Illykh, P.A., Shen, X., Huang, K., et al. (2018). Broadly neutralizing antibodies from human survivors target a conserved site in the Ebola virus glycoprotein HR2-MPER region. *Nat. Microbiol.* 3, 670–677.
- Furuyama, W., Marzi, A., Nanbo, A., Haddock, E., Maruyama, J., Miyamoto, H., Igarashi, M., Yoshida, R., Noyori, O., Feldmann, H., and Takada, A. (2016). Discovery of an antibody for pan-ebolavirus therapy. *Sci. Rep.* 6, 20514.
- Gilchuk, P., Kuzmina, N., Illykh, P.A., Huang, K., Gunn, B.M., Bryan, A., Davidson, E., Doranz, B.J., Turner, H.L., Fusco, M.L., et al. (2018). Multifunctional Pan-ebolavirus Antibody Recognizes a Site of Broad Vulnerability on the Ebo-lavirus Glycoprotein. *Immunity* 49, 363–374.
- Gunn, B.M., Yu, W.H., Karim, M.M., Brannan, J.M., Herbert, A.S., Wec, A.Z., Halfmann, P.J., Fusco, M.L., Schendel, S.L., Gangavarapu, K., et al. (2018). A Role for Fc Function in Therapeutic Monoclonal Antibody-Mediated Protection against Ebola Virus. *Cell Host Microbe* 24, 221–233.
- Guo, J., Zuo, T., Cheng, L., Wu, X., Tang, J., Sun, C., Feng, L., Chen, L., Zhang, L., and Chen, Z. (2015). Simian immunodeficiency virus infection evades vaccine-elicited antibody responses to V2 region. *J. Acquir. Immune Defic. Syndr.* 68, 502–510.
- Hashiguchi, T., Fusco, M.L., Bornholdt, Z.A., Lee, J.E., Flyak, A.I., Matsuoka, R., Kohda, D., Yanagi, Y., Hammel, M., Crowe, J.E., Jr., and Saphire, E.O. (2015). Structural basis for Marburg virus neutralization by a cross-reactive human antibody. *Cell* 160, 904–912.
- Holtsberg, F.W., Shulenin, S., Vu, H., Howell, K.A., Patel, S.J., Gunn, B., Karim, M., Lai, J.R., Frei, J.C., Nyakatura, E.K., et al. (2015). Pan-ebolavirus and Pan-filovirus Mouse Monoclonal Antibodies: Protection against Ebola and Sudan Viruses. *J. Virol.* 90, 266–278.
- Howell, K.A., Brannan, J.M., Bryan, C., McNeal, A., Davidson, E., Turner, H.L., Vu, H., Shulenin, S., He, S., Kuehne, A., et al. (2017). Cooperativity Enables Non-neutralizing Antibodies to Neutralize Ebovirus. *Cell Rep.* 19, 413–424.
- Huang, K.Y., Rijal, P., Schimanski, L., Powell, T.J., Lin, T.Y., McCauley, J.W., Daniels, R.S., and Townsend, A.R. (2015). Focused antibody response to influenza linked to antigenic drift. *J. Clin. Invest.* 125, 2631–2645.
- Huang, K.A., Rijal, P., Jiang, H., Wang, B., Schimanski, L., Dong, T., Liu, Y.M., Chang, P., Iqbal, M., Wang, M.C., et al. (2019). Structure-function analysis of neutralizing antibodies to H7N9 influenza from naturally infected humans. *Nat. Microbiol.* 4, 306–315.
- Jackson, K.J., Liu, Y., Roskin, K.M., Glanville, J., Hoh, R.A., Seo, K., Marshall, E.L., Gurley, T.C., Moody, M.A., Haynes, B.F., et al. (2014). Human responses to influenza vaccination show seroconversion signatures and convergent antibody rearrangements. *Cell Host Microbe* 16, 105–114.
- Keck, Z.Y., Enterlein, S.G., Howell, K.A., Vu, H., Shulenin, S., Warfield, K.L., Froude, J.W., Araghi, N., Douglas, R., Biggins, J., et al. (2015). Macaque Monoclonal Antibodies Targeting Novel Conserved Epitopes within Filovirus Glycoprotein. *J. Virol.* 90, 279–291.
- Kozak, R., He, S., Kroeker, A., de La Vega, M.A., Audet, J., Wong, G., Urfano, C., Antonian, K., Embury-Hyatt, C., Kobinger, G.P., and Qiu, X. (2016). Ferrets Infected with Bundibugyo Virus or Ebola Virus Recapitulate Important Aspects of Human Filovirus Disease. *J. Virol.* 90, 9209–9223.
- Kroeker, A., He, S., de La Vega, M.A., Wong, G., Embury-Hyatt, C., and Qiu, X. (2017). Characterization of Sudan Ebovirus infection in ferrets. *Oncotarget* 8, 46262–46272.
- Kugelman, J.R., Kugelman-Tonos, J., Ladner, J.T., Pettit, J., Keeton, C.M., Nagle, E.R., Garcia, K.Y., Froude, J.W., Kuehne, A.I., Kuhn, J.H., et al. (2015). Emergence of Ebola Virus Escape Variants in Infected Nonhuman Primates Treated with the MB-003 Antibody Cocktail. *Cell Rep.* 12, 2111–2120.
- Kuhn, J.H., Lofts, L.L., Kugelman, J.R., Smither, S.J., Lever, M.S., van der Groen, G., Johnson, K.M., Radoshitzky, S.R., Bavari, S., Jahrling, P.B., et al. (2014). Reidentification of Ebola Virus E718 and ME as Ebola Virus/H.sapiens-tc/COD/1976/Yambuku-Ecran. *Genome Announc.* 2, e01178–14.
- Lee, J.E., Fusco, M.L., Hessel, A.J., Oswald, W.B., Burton, D.R., and Saphire, E.O. (2008). Structure of the Ebola virus glycoprotein bound to an antibody from a human survivor. *Nature* 454, 177–182.
- Linderman, S.L., Chambers, B.S., Zost, S.J., Parkhouse, K., Li, Y., Herrmann, C., Ellebedy, A.H., Carter, D.M., Andrews, S.F., Zheng, N.Y., et al. (2014). Potential antigenic explanation for atypical H1N1 infections among middle-aged adults during the 2013–2014 influenza season. *Proc. Natl. Acad. Sci. USA* 111, 15798–15803.
- Maruyama, T., Rodriguez, L.L., Jahrling, P.B., Sanchez, A., Khan, A.S., Nichol, S.T., Peters, C.J., Parren, P.W., and Burton, D.R. (1999). Ebola virus can be effectively neutralized by antibody produced in natural human infection. *J. Virol.* 73, 6024–6030.
- Marzi, A., Yoshida, R., Miyamoto, H., Ishijima, M., Suzuki, Y., Higuchi, M., Matsuyama, Y., Igarashi, M., Nakayama, E., Kuroda, M., et al. (2012). Protective efficacy of neutralizing monoclonal antibodies in a nonhuman primate model of Ebola hemorrhagic fever. *PLoS ONE* 7, e36192.
- Matrosovich, M., Matrosovich, T., Carr, J., Roberts, N.A., and Klenk, H.D. (2003). Overexpression of the alpha-2,6-sialyltransferase in MDCK cells increases influenza virus sensitivity to neuraminidase inhibitors. *J. Virol.* 77, 8418–8425.
- Miller, E.H., Obernosterer, G., Raaben, M., Herbert, A.S., Deffieu, M.S., Krishnan, A., Ndungo, E., Sandesara, R.G., Carette, J.E., Kuehne, A.I., et al. (2012). Ebola virus entry requires the host-programmed recognition of an intracellular receptor. *EMBO J.* 31, 1947–1960.
- Misasi, J., Gilman, M.S., Kanekiyo, M., Gui, M., Cagigi, A., Mulangu, S., Corti, D., Ledgerwood, J.E., Lanzavecchia, A., Cunningham, J., et al. (2016). Structural and molecular basis for Ebola virus neutralization by protective human antibodies. *Science* 351, 1343–1346.
- Murin, C.D., Fusco, M.L., Bornholdt, Z.A., Qiu, X., Olinger, G.G., Zeitlin, L., Kobinger, G.P., Ward, A.B., and Saphire, E.O. (2014). Structures of protective antibodies reveal sites of vulnerability on Ebola virus. *Proc. Natl. Acad. Sci. USA* 111, 17182–17187.

- Oropallo, M.A., and Cerutti, A. (2014). Germinal center reaction: antigen affinity and presentation explain it all. *Trends Immunol.* 35, 287–289.
- Pappas, L., Foglierini, M., Piccoli, L., Kallewaard, N.L., Turrini, F., Silacci, C., Fernandez-Rodriguez, B., Agatic, G., Giacchetto-Sasselli, I., Pellicciotta, G., et al. (2014). Rapid development of broadly influenza neutralizing antibodies through redundant mutations. *Nature* 516, 418–422.
- Parameswaran, P., Liu, Y., Roskin, K.M., Jackson, K.K., Dixit, V.P., Lee, J.Y., Artiles, K.L., Zompi, S., Vargas, M.J., Simen, B.B., et al. (2013). Convergent antibody signatures in human dengue. *Cell Host Microbe* 13, 691–700.
- Pascal, K.E., Dudgeon, D., Trefry, J.C., Anantpadma, M., Sakurai, Y., Murin, C.D., Turner, H.L., Fairhurst, J., Torres, M., Rafique, A., et al. (2018). Development of clinical-stage human monoclonal antibodies that treat advanced Ebola virus disease in nonhuman primates. *J. Infect. Dis.* 218 (Suppl 5), S612–S626.
- Pettitt, J., Zeitlin, L., Kim, D.H., Working, C., Johnson, J.C., Bohorov, O., Bratcher, B., Hiatt, E., Hume, S.D., Johnson, A.K., et al. (2013). Therapeutic intervention of Ebola virus infection in rhesus macaques with the MB-003 monoclonal antibody cocktail. *Sci. Transl. Med.* 5, 199ra113.
- Qiu, X., Fernando, L., Melito, P.L., Audet, J., Feldmann, H., Kobinger, G., Alimonti, J.B., and Jones, S.M. (2012). Ebola GP-specific monoclonal antibodies protect mice and guinea pigs from lethal Ebola virus infection. *PLoS Negl. Trop. Dis.* 6, e1575.
- Qiu, X., Wong, G., Audet, J., Bello, A., Fernando, L., Alimonti, J.B., Fausther-Bovendo, H., Wei, H., Aviles, J., Hiatt, E., et al. (2014). Reversion of advanced Ebola virus disease in nonhuman primates with ZMapp. *Nature* 514, 47–53.
- Saphire, E.O., and Aman, M.J. (2016). Feverish Quest for Ebola Immunotherapy: Straight or Cocktail? *Trends Microbiol.* 24, 684–686.
- Saphire, E.O., Schendel, S.L., Fusco, M.L., Gangavarapu, K., Gunn, B.M., Wec, A.Z., Halfmann, P.J., Brannan, J.M., Herbert, A.S., Qiu, X., et al. (2018). Systematic Analysis of Monoclonal Antibodies against Ebola Virus GP Defines Features that Contribute to Protection. *Cell* 174, 938–952.
- Schmidt, A.G., Xu, H., Khan, A.R., O'Donnell, T., Khurana, S., King, L.R., Manischewitz, J., Golding, H., Suphaphiphat, P., Carfi, A., et al. (2013). Pre-configuration of the antigen-binding site during affinity maturation of a broadly neutralizing influenza virus antibody. *Proc. Natl. Acad. Sci. USA* 110, 264–269.
- Schornberg, K., Matsuyama, S., Kabsch, K., Delos, S., Bouton, A., and White, J. (2006). Role of endosomal cathepsins in entry mediated by the Ebola virus glycoprotein. *J. Virol.* 80, 4174–4178.
- Shedlock, D.J., Bailey, M.A., Popernack, P.M., Cunningham, J.M., Burton, D.R., and Sullivan, N.J. (2010). Antibody-mediated neutralization of Ebola virus can occur by two distinct mechanisms. *Virology* 401, 228–235.
- Stanley, D.A., Honko, A.N., Asiedu, C., Trefry, J.C., Lau-Kilby, A.W., Johnson, J.C., Hensley, L., Ammendola, V., Abbate, A., Grazioli, F., et al. (2014). Chimpanzee adenovirus vaccine generates acute and durable protective immunity against ebolavirus challenge. *Nat. Med.* 20, 1126–1129.
- Takada, A., Ebihara, H., Jones, S., Feldmann, H., and Kawaoka, Y. (2007). Protective efficacy of neutralizing antibodies against Ebola virus infection. *Vaccine* 25, 993–999.
- Thornburg, N.J., Zhang, H., Bangaru, S., Sapparapu, G., Kose, N., Lamplé, R.M., Bombardi, R.G., Yu, Y., Graham, S., Branchizio, A., et al. (2016). H7N9 influenza virus neutralizing antibodies that possess few somatic mutations. *J. Clin. Invest.* 126, 1482–1494.
- Tickle, S., Howells, L., O'Dowd, V., Starkie, D., Whale, K., Saunders, M., Lee, D., and Lightwood, D. (2015). A fully automated primary screening system for the discovery of therapeutic antibodies directly from B cells. *J. Biomol. Screen.* 20, 492–497.
- Tiller, T., Meffre, E., Yurasov, S., Tsuiji, M., Nussenzweig, M.C., and Wardemann, H. (2008). Efficient generation of monoclonal antibodies from single human B cells by single cell RT-PCR and expression vector cloning. *J. Immunol. Methods* 329, 112–124.
- Trombley, A.R., Wachter, L., Garrison, J., Buckley-Beason, V.A., Jahrling, J., Hensley, L.E., Schoepp, R.J., Norwood, D.A., Goba, A., Fair, J.N., and Kulesh, D.A. (2010). Comprehensive panel of real-time TaqMan polymerase chain reaction assays for detection and absolute quantification of filoviruses, arenaviruses, and New World hantaviruses. *Am. J. Trop. Med. Hyg.* 82, 954–960.
- Wec, A.Z., Herbert, A.S., Murin, C.D., Nyakatura, E.K., Abelson, D.M., Fels, J.M., He, S., James, R.M., de la Vega, M.A., Zhu, W., et al. (2017). Antibodies from a Human Survivor Define Sites of Vulnerability for Broad Protection against Ebolaviruses. *Cell* 169, 878–890.
- West, B.R., Wec, A.Z., Moyer, C.L., Fusco, M.L., Ilinykh, P.A., Huang, K., James, R.M., Herbert, A.S., Hui, S., Wirchnianski, A.S., et al. (2018). Structural Basis of Broad Ebolavirus Neutralization by a Human Survivor Antibody. *bioRxiv*. <https://doi.org/10.1101/394502>.
- Wilson, J.A., Hevey, M., Bakken, R., Guest, S., Bray, M., Schmaljohn, A.L., and Hart, M.K. (2000). Epitopes involved in antibody-mediated protection from Ebola virus. *Science* 287, 1664–1666.
- Wrammert, J., Smith, K., Miller, J., Langley, W.A., Kokko, K., Larsen, C., Zheng, N.Y., Mays, I., Garman, L., Helms, C., et al. (2008). Rapid cloning of high-affinity human monoclonal antibodies against influenza virus. *Nature* 453, 667–671.
- Wrammert, J., Koutsouanos, D., Li, G.M., Edupuganti, S., Sui, J., Morrissey, M., McCausland, M., Skountzou, I., Hornig, M., Lipkin, W.I., et al. (2011). Broadly cross-reactive antibodies dominate the human B cell response against 2009 pandemic H1N1 influenza virus infection. *J. Exp. Med.* 208, 181–193.
- Xiao, J.H., Rijal, P., Schimanski, L., Tharakeswar, A.K., Wright, E., Annaert, W., and Townsend, A. (2018). Characterization of Influenza Virus Pseudotyped with Ebolavirus Glycoprotein. *J. Virol.* 92, e00941–1.
- Zhao, X., Howell, K.A., He, S., Brannan, J.M., Wec, A.Z., Davidson, E., Turner, H.L., Chiang, C.I., Lei, L., Fels, J.M., et al. (2017). Immunization-Elicited Broadly Protective Antibody Reveals Ebolavirus Fusion Loop as a Site of Vulnerability. *Cell* 169, 891–904.
- Zinkernagel, R.M. (2002). Uncertainties - discrepancies in immunology. *Immunol. Rev.* 185, 103–125.
- Zuo, T., Shi, X., Liu, Z., Guo, L., Zhao, Q., Guan, T., Pan, X., Jia, N., Cao, W., Zhou, B., et al. (2011). Comprehensive analysis of pathogen-specific antibody response in vivo based on an antigen library displayed on surface of yeast. *J. Biol. Chem.* 286, 33511–33519.

STAR★METHODS

KEY RESOURCES TABLE

REAGENT or RESOURCE	SOURCE	IDENTIFIER
Antibodies		
c13C6	Wilson et al., 2000	N/A
c2G4	Wilson et al., 2000	N/A
c4G7	Wilson et al., 2000	N/A
6D6	Furuyama et al., 2016	N/A
mAb100	Corti et al., 2016	N/A
mAb114	Corti et al., 2016	N/A
KZ52	Maruyama et al., 1999	PDB: 3CSY
ZMapp cocktail	Mapp Biopharmaceutical	N/A
anti-CD27 PE-Cy7	BD PharMingen	Cat#560609; RRID: AB_1727456
anti-CD19 FITC	BD PharMingen	Cat#555412; RRID: AB_395812
anti-CD3 PB	BD PharMingen	Cat#558117; RRID: AB_397038
anti-CD20 APC-H7	BD PharMingen	Cat#560734; RRID: AB_1727449
anti-CD38 PE-Cy5	BD PharMingen	Cat#555461; RRID: AB_395854
anti-IgG BV605	BD PharMingen	Cat#563246; RRID: AB_2738092
Extravidin-R-Phycoerythrin	Sigma	Cat#E4011
HRP-conjugated Rabbit anti-human IgG	DakoCytomation	Cat#P0214
HRP-conjugated Streptavidin	DakoCytomation	Cat#P0397
Alexafluor 647-conjugated Goat anti-human IgG	Thermo Fisher	Cat#A21445
FITC-conjugated Goat anti-human IgG	Life Technologies	Cat#H10301
Rabbit anti-EBOV GP pAb	IBT Bioservices	Cat#0301-015
Bacterial and Virus Strains		
EBOV GP (in ChAd3-EBOV GP vaccine)	Stanley et al., 2014	GenBank: AF086833
EBOV GP (in MVA-BN Filo vaccine)	Patent: WO2016036955A1	GenBank: ABX75367.1
SUDV GP (in MVA-BN Filo vaccine)	Patent: WO2016036955A1	GenBank: AAU43887.1
MARV GP (in MVA-BN Filo vaccine)	Patent: WO2016036955A1	GenBank: ABA87127.1
TAFV NP (in MVA-BN Filo vaccine)	Patent: WO2016036955A1	GenBank: ACI28629.1
GP EBOV/ H.sapiens-wt/GIN/2014/Makona-Kissidougou-C15	(Xiao et al., 2018) This paper	GenBank: KJ660346.2
GP EBOV/H.sap-tc/COD/76/Zaire-Mayinga	(Xiao et al., 2018) This paper	GenBank: AF086833.2
GP SUDV/ H.sapiens-tc/UGA/2000/Gulu-808892	(Xiao et al., 2018) This paper	GenBank: NC006432.1
Guinea pig-adapted EBOV EBOV/H.sapiens-tc/COD/1976/Yambuku-Ecran	(Dowall et al., 2014) PHE, Porton Down, UK	GenBank: KM655246.1
DH5 α Competent <i>E. coli</i> (High Efficiency)	NEB	Cat#C2987
Gibson Assembly Master Mix	NEB	Cat#E2611
Biological and Chemical Samples		
Human PBMCs; a week after boost immunization	Ewer et al., 2016	N/A
Chemicals, Peptides and Recombinant Proteins		
Phosphate buffered saline (PBS)	Oxoid	Cat#BR0014G
Penicillin/Streptomycin	Sigma	Cat#P0781
L-Glutamine	Sigma	Cat#G7513
DMEM	Sigma	Cat#D5796
RPMI	Sigma	Cat#R8758
Heat Inactivated Fetal Bovine Serum (FBS)	Sigma	Cat#F9665

(Continued on next page)

Continued

REAGENT or RESOURCE	SOURCE	IDENTIFIER
BSA for Viral Growth Medium	Sigma	Cat#A8327
BSA as Blocker in FACS Buffer	Thermo Fisher	Cat#37525
MES hydrate	Sigma	Cat#M2933
HEPES buffer	GIBCO	Cat#15630-056
Thermolysin	Sigma	Cat#P1512
Protein A Sepharose	Sigma	Cat#P3391
Extravidin Peroxidase	Sigma	Cat#E2886
Alexa Fluor 647 conjugated Streptavidin	Thermo Fisher	Cat#S21374
OPD Substrate	Sigma	Cat#P9187
Yeast phage peptide library	This paper	N/A
Capture Select C-tag Affinity matrix	Thermo Fisher	Cat#191307005
Commercial kits		
QIAquick gel extraction kit	QIAGEN	Cat#28706
QIAprep Spin Miniprep kit	QIAGEN	Cat#27106
Plasmid maxiprep kit	QIAGEN	Cat#12362/ 12963
QIAquick PCR purification kit	QIAGEN	Cat#28106
QIAprep 96 Turbo Miniprep Kit	QIAGEN	Cat#27191
QIAquick 96 PCR Purification Kit	QIAGEN	Cat#28181
RNeasy Mini kit	QIAGEN	Cat#74104
EZ-link Sulfo-NHS-LC-biotin	Life Technologies	Cat#21327
Amicon-Ultra 15 Centrifugal Unit	Millipore	Cat#UFC903096
Expi293 Expression System	Thermo Fisher	Cat#A14635
Deposited Data		
mAb sequences	GenBank, NCBI	Accession numbers: MK552329 – MK552374
Experimental Models: Cell Lines		
Human: HEK293T cells	Dunn School, Oxford	N/A
Human: Expi293F cells	Life Technologies	Cat#A14527
Dog: MDCK-SIAT1 cells	Matrosovich et al., 2003	ECACC 05071502
Experimental Models: Organisms/Strains		
Guinea Pig: HsdDhl	Marshall BioResources/Envigo	Item No. 45903F
Software and Algorithms		
PRISM	GraphPad Software Version 7	https://www.graphpad.com
Pymol	Schrodinger LLC Version 2.0.6	https://pymol.org/2/
MEGA Alignment and Phylogeny	MEGA Version 7.0	https://www.megasoftware.net/
FlowJo	Treestar, Version 10	https://www.flowjo.com/
BIAevaluation Software	GE Healthcare Version 4.1.1	N/A
Other		
IMGT/V-quest	IMGT	http://www.imgt.org
Production of antibodies used for Guinea Pig protection	Absolute Antibody Ltd.	N/A

CONTACT FOR REAGENT AND RESOURCE SHARING

Further information and requests for resources and reagents should be directed and will be fulfilled by the Lead Contact, Alain Townsend (alain.townsend@imm.ox.ac.uk). Distribution of patented antibodies will require signing an MTA in accordance with policies of University of Oxford.

EXPERIMENTAL MODEL AND SUBJECT DETAILS

Ethics Statement

Human PBMC samples used here are from the EBL01 study described in detail in [Ewer et al. \(2016\)](#). The study received ethical approval from the United Kingdom National Research Ethics Service, the Committee South Central-Oxford A (reference 14/SC/1256), Committee South Central – Oxford A (OXREC A; Ref: 14/SC/1256), the Medicines and Healthcare products Regulatory Agency (MHRA; Ref: 21584/0334/001-0001) and the Oxford University Clinical Trials and Research Governance team, who monitored GCP compliance. An independent Data Safety Monitoring Board (DSMB) provided safety oversight. The volunteers signed written consent forms and consent was verified before each vaccination.

Animal studies were performed under Containment Level 4 conditions with all procedures being undertaken according to the United Kingdom Animals (Scientific Procedures) Act 1986. Studies were conducted under Establishment License reference PEL PCD 70/1707 with Project License PPL 30/3247. Studies were approved by the Public Health England ethics committee and the Project License approved by a UK Home Office inspector.

Human PBMC

PBMC samples were obtained from the human vaccinees who received ChAd3 EBOZ vaccine and booster dose of MVA-BN Filo ([Table S5](#)), as a part of EBL01 trial ([Ewer et al., 2016](#)). The vaccine components are included in Key Resources table. Participants were healthy adults between the ages of 18 and 50 years. The study included approximately equal numbers of male and female participants. However, our study was blinded to age and gender of the 11 volunteers who donated samples for isolation of antibodies.

Guinea Pigs challenge studies

Thirty-six female Dunkin Hartley guinea pigs (HsdDhl) weighing between 220–300 g (3–5 weeks old), were purchased from a UK home office approved breeder and supplier (Marshall BioResources). Guinea pigs were cared for and handled in the category 4 lab at Public Health England, Porton Down, according to the guidelines for the species. Animals were monitored at least once a day for food and water consumption and given environmental enrichment relevant to the species. Cages were cleaned out completely at least once a week with a complete bedding material change. Animals were kept in pairs and were randomly assigned to experimental groups prior to the start of the study. The guinea pigs were implanted with a temperature and identity chip during a five-day acclimatization period.

All guinea pigs were challenged with 10^3 TCID₅₀ of guinea pig adapted Ebola virus in a volume of 200 μ L via the subcutaneous route. During the course of the study, weights and temperatures were collected at least once daily and clinical scores assessed at least twice a day. Animals which met predefined endpoints (20% weight loss; 10% weight and moderate clinical signs; or immobility) were culled by a Schedule 1 approved method. Antibody cocktails were prepared a day before administration. Antibodies were delivered 3 days post-challenge via the intraperitoneal route in a volume of 2 mL ($n = 6$ /group). As a positive control, ZMapp was given in a dose of 5 mg/Kg per animal. Untreated animals were given 2 mL PBS.

Cell Lines

HEK293T (human embryonic kidney) was obtained from the Sir William Dunn School of Pathology, Oxford, and MDCK-SIAT1 (Madin Darby Canine kidney – sialltransferase) cells were obtained from ATCC. Both the cell lines were cultured in Dulbecco's Modified Eagle Medium (DMEM) supplemented with 10% fetal bovine serum, 2 mM glutamine, 100 I.U./mL penicillin and 100 μ g/mL streptomycin. They were incubated at 37°C with 5% CO₂. Expi293F cells were purchased from Life Technologies and used according to manufacturer's protocol. Viruses were expanded in MDCK-SIAT1 cells transduced to express various Ebola GPs in Virus Growth Medium (VGM; DMEM supplemented with 0.1% BSA, 2 mM glutamine, 100 I.U./mL penicillin and 100 μ g/mL streptomycin, and 10mm HEPES buffer).

MDCK-SIAT cells expressing Ebola GP and MLD-deleted GP

The codon optimized GP gene sequences were ordered from Geneart. The GP genes were cloned in to a Lenti virus vector pHR-SIN ([Demaision et al., 2002](#)). MDCK-SIAT1 cell lines ([Matrosovich et al., 2003](#)) were transduced with disabled Lenti virus produced in HEK293T cells to express the glycoprotein. Transduced cells were stained with specific mAbs and FACS sorted for maximal surface expression. MLD-deleted GP had amino acids 313–463 removed.

Viruses

Ebola pseudotyped influenza viruses (S-FLU) were generated as previously described in detail ([Xiao et al., 2018](#)). Human codon optimized cDNA encoding Ebola virus glycoproteins (mentioned in [Key Resources Table](#)) were synthesized by Geneart, Life Technologies. Influenza pseudotyped viruses were propagated and grown in MDCK-SIAT1 cell lines transduced with disabled lentivirus to express the surface Ebola virus glycoprotein. These viruses were titrated using the expression of eGFP as a reporter. The virus was titrated to give at least a 4 fold difference between infected and uninfected cells.

Ebola virus (strain Yambuku-Ecran, previously known as ME718 ([Kuhn et al., 2014](#)) adapted to cause lethal disease in guinea pigs through sequential passage. The virus was passaged five times to achieve lethality in guinea pigs ([Dowall et al., 2014](#)).

METHOD DETAILS

Isolation of mAbs from plasmablasts

Antibodies were isolated by FACS sorting, PCR and antibody variable gene cloning of a single B cell plasmablast from eight vaccinated human individuals using the previously described methods (Tiller et al., 2008; Wrammert et al., 2008), with a few modifications. Briefly, PBMC were incubated with a cocktail of antibodies to CD3 (PB; UCHT1; BD PharMingen), CD20 (APC-H7; 2H7; BD PharMingen), CD19 (FITC; H1B19; BD PharMingen), CD27 (PE-Cy7, M-T271; BD PharMingen), CD38 (PE-Cy5, HIT2; BD PharMingen) and IgG (BV605, G18-145; BD PharMingen). For a few sorts, Ebola GP protein (10 μ g/mL) and a known biotin-labeled anti-MLD antibody (10 μ g/mL) were used to sort antigen specific B cell plasmablasts. Single cells with the phenotype of CD3⁺ CD20^{low}, CD19⁺, CD27⁺, CD38⁺, IgG⁺ were sorted on a FACS Aria III cell sorter (BD Biosciences). Single cells were sorted into 96-well PCR plates containing lysis buffer followed by single cell RT-PCR. Nested PCR was slightly modified to existing methods. Overlapping bases (approx. 20 nucleotides) were added on to existing 5' and 3' primers without interfering the restriction sites, which could be used as a back-up, to enable digestion free Gibson cloning. PCR products were purified in a QIAGEN 96-well system and the inserts were assembled with cut plasmid in the Gibson mix (NEB). Two μ L of assembled product was used to transform 10 μ L DH5 α E. Coli (NEB, C2987) in 96-well plates. Three colonies for each heavy and light chain were grown in a 96-well plate format and purified using QIAGEN Turbo 96 miniprep kit. Plasmids were eluted using 100 μ L TE buffer. Transfection of 293T cells with heavy and light plasmids (~200 ng of each with 120 μ g/mL linear PEI, in 250 μ L total volume) and immunofluorescence assays were also performed in a 96-well tissue culture plate.

Isolation of mAbs from memory B cells

PBMCs harvested 28 days after vaccination boost from three volunteers was collected. B cell culture screening was performed using a method similar to that described by Tickle et al. (2015). Human B cell cultures were prepared using 132 \times 96-well plates at a cell density of approximately 5000 cells per well. After 7-days culture, screening was performed. Briefly, the presence of Ebola glycoprotein-binding antibodies in B cell culture supernatants was determined using a homogeneous fluorescence-based binding assay performed on a Applied Biosystems 8200 cellular detection system device using MDCK cells stably transfected to express surface Ebola glycoprotein. Binding was revealed with a goat anti-human IgG Fc γ -specific Dylight 649 conjugate (Jackson). Following primary screening, positive supernatants containing reactive antibody were consolidated on 96-well bar-coded master plates and B cells in cell culture plates frozen at -80° C. Master plates were then screened in a further homogeneous fluorescence binding assay to confirm that the antibodies bound the Ebola glycoprotein-expressing MDCK-SIAT1 cells and not the parental MDCK-SIAT1 cells.

The Fluorescent Foci method (US Patent 7993864/ Europe EP1570267B1) (Clargo et al., 2014) utilizing Ebola glycoprotein-expressing MDCK-SIAT1 cells was used to identify and isolate antigen-specific B cells from positive wells, and specific antibody variable region genes were recovered from single cells by reverse transcription (RT)-PCR using heavy and light chain variable region-specific primers. PCR primers contained restriction sites at the 3' and 5' ends allowing cloning of the variable region into a human IgG1 (V_H), human kappa (V_K) or human lambda (V_L) mammalian expression vector. Heavy and light chain constructs were co-transfected into Expi293F cells using Expifectamine 293 (Thermo Fisher) and recombinant antibody expressed. After 6 days expression, supernatants were harvested, and antibody rescreened for selectivity using the specificity assays described above. Antibody was purified from conditioned media using affinity chromatography and characterized further.

Immunofluorescence Binding Assays

Immunofluorescence assay was done to screen the binding of antibodies in culture supernatant to Ebola glycoprotein. A 96-well plate was coated overnight with stable transduced MDCK-SIAT1 cells expressing Ebola glycoprotein (E-SIAT cells). Antibody supernatant (50 μ L) was incubated with a monolayer of E-SIAT cells. After 1 h incubation at RT, plates were washed with PBS. A secondary antibody goat anti-human IgG conjugated with Alexa Fluor647 (A21445; Thermo Fisher; 1:400) or FITC (H10301; Life technologies; 1:160) was added to wells and let incubate for 1 h in dark. Plates were then washed with PBS and fixed with 1% formalin. Fluorescence was observed under the fluorescence microscope and quantified using the Clariostar plate reader (BMG Labtech). GP binding antibodies and influenza antibodies were used as positive and negative controls respectively.

Expression and Purification of Antibody

Antibodies were expressed in HEK293 or Expi293F cells (Thermo Fisher) by co-transfection with heavy and light plasmids. Antibodies were purified from harvested cell supernatant using protein A Sepharose (P3391; Sigma) or MabSelect SuRe (GE Healthcare, 17-5438-01). The column was washed with Tris buffered saline (TBS) and eluted with sodium citrate buffer pH 3.0–3.4. Elution pools were neutralised with 2 M Tris/HCl pH 8.0 and absorbance read at 280 nm. Samples were then buffer exchanged into PBS pH 7.4 using Amicon Ultra Spin columns with a 30K cut off membrane (Millipore, UFC903096) and centrifugation at 4000 g.

mAbs used for guinea pig protection were expressed in 293T cells and affinity purified by the Absolute Antibody Ltd. and provided at 15 mg/mL which were aliquoted and kept at -80° C until used.

Expression and purification of soluble glycoproteins

EBOV GP (aa1-650 only; aa650-676 deleted) with four amino acid C-tag (EPEA) at C terminus was expressed in HEK293E cells (2×10^6 cells/mL) using PEI transfection. Cells were incubated at 37°C, 8.6% CO₂, 130 rpm for 6 days in Expi293 expression media (GIBCO). Supernatant was concentrated by tangential flow filtration and 10 kDa membrane (Millipore). Glycoprotein was purified by affinity chromatography using CaptureSelect C-tag Affinity Matrix (Thermo Fisher), eluted in 2 M MgCl₂, 20 mM Tris, pH 7.4; followed by size exclusion chromatography in tris-buffered saline using a HiLoad Superdex16/600 200 pg column (GE Healthcare).

Virus Neutralisation Assays

Neutralisation assays were done as previously described (Xiao et al., 2018). Ebola pseudotyped influenza virus (E-S-FLU) diluted in virus growth medium (VGM) was incubated with mAbs in serial dilution in PBS for 2 h at 37°C. Antibodies and virus both were in 50 µL volume. After 2 hours, 100 µL of MDCK-SIAT1 cells (3×10^4) diluted in VGM were then added to each well. Cells were incubated for 20–24 h at 37°C, 5% CO₂. Next day, the medium was removed from the well and the cells were fixed with 10% formalin for at least 30 min after which the wells were washed with PBS and stored in 100 µL PBS at 4°C. Once fixed, the plates can be read anytime. The eGFP signal was found to be stable up to six months as long as the plate has not dried. The eGFP fluorescence was read using the Clariostar plate reader (BMG Labtech). The settings in Clariostar plate reader were: fluorescence excitation at 483 nm (bandwidth of 8 nm), emission at 515 nm (bandwidth of 8 nm) with a 499-nm dichroic filter. Each well had 50 flashes at a 4-mm diameter and fluorescence readout from the top optic, giving the orbital averaging value. The gain was fixed to 2000 and the focal-length was adjusted for every experiment, which was between 4.5 – 5.5. Virus only and medium only controls for maximum and minimum signals were included. Percent infection was calculated based on the wells containing virus only and medium only. Inhibitory concentration at 50% and 90% was derived by linear interpolation.

Epitope Mapping using Competitive Binding Assays

Competition binding assay was performed to find out if a known/reference antibody with a defined binding site is blocked by the testing antibody and vice versa. Antibody was biotinylated using EZ-link Sulfo-NHS-LC-biotin (21327; Life Technologies). Biotin-labeled antibody and competing mAb (in 10-fold excess over biotin-mAb) were mixed and transferred to a monolayer of E-SIAT cells. After 1 h incubation, cells were washed. A second layer of Extravidin-FITC (E2761; Sigma; 1:400) or Extravidin Peroxidase (E2886; Sigma; 1:1600) or Streptavidin-Alexa Fluor 647 (S21374; Thermo Fisher; 1:400) was then added for 1 hour. Cells were washed three times and then binding was detected. When using a fluorescent second layer, cells were fixed in 1% formalin and fluorescence was quantified on the Clariostar Plate reader. When Extravidin-Peroxidase was used, signal was developed by adding OPD substrate (P9187; Sigma) and the reaction stopped with 50 µL 1 M H₂SO₄. We found Streptavidin Alexa Fluor 647 preferable because it gave a better signal to background ratio in the plate reader. Mean and 90% confidence interval of eight replicate measurements were calculated. Self-blocking (minimum signal), PBS (background fluorescence) and a non-competing antibody (influenza mAb or a mAb to the mucin-like domain; maximum signal) were used as controls. The competition was measured as: $(X - \text{Min binding}) / (\text{Maximum binding} - \text{Minimum binding})$, where X = Binding of the biotinylated mAb in presence of competing mAb, Minimum binding = Blocking of the biotinylated mAb by self or background binding, Maximum binding = Binding of biotinylated mAb in presence non-competing mAb.

Epitope Mapping using Yeast Peptide-Display Assays

Epitope mapping of the mAbs was carried out based on the yeast surface display (YSD) library as previously described (Zuo et al., 2011; Guo et al., 2015). Briefly, the combinatorial fragment library of Zaire Ebola GP was constructed and displayed on the surface of yeast for antibody staining and Fluorescence-activated cell sorting (FACS). Specifically, the full-length GP gene was digested and PCR-reassembled into a range of 100–900 bp fragments, the reassembled fragments were gel purified and cloned into yeast surface display vector. The cloned products were then transformed into competent yeast cell line EBY100 using electroporation. The yeast library was induced and incubated with each of the Ebola mAbs and positive sorted by FACS using Aria III (BD, USA). The sorted positive yeast clones displaying the respective antigenic fragments were harvested and the plasmids encoding the corresponding fragments were extracted and subjected to sequencing and sequence analysis.

Binding Kinetics using Surface Plasmon Resonance (SPR)

Binding kinetics of antibodies to both monomeric and trimeric Ebola virus glycoprotein ectodomain was assessed by SPR using a Biacore 3000 instrument (GE Healthcare), whereby antibody was captured on a CM5 chip (GE Healthcare) via immobilized anti-human IgG Fc specific polyclonal antibody, followed by successive titration of glycoprotein. Resulting sensorgrams were analyzed to determine association and dissociation rate constants over a range of GP concentrations.

Affinity purified polyclonal goat F(ab)₂ anti-human IgG Fc (Jackson, 109-006-098) was immobilized following activation of test and reference flow cells by injection of 50 µL of a fresh mixture of 50 mM N-hydroxysuccinimide and 200 mM 1-ethyl-3-(3-dimethylaminopropyl)-carbodiimide at a flow rate of 10 µL/min. Polyclonal at 50 µg/mL in 10 mM acetate pH 5.0 buffer was injected (50 µL) over the test flow cell and both test and reference flow cell surfaces were then deactivated with a 50 µL pulse of 1 M ethanolamine.HCl pH 8.5.

Binding assays were carried out at 25°C in HBS-EP running buffer (10 mM HEPES, pH 7.4, 150 mM NaCl, 3 mM EDTA, 0.05% Surfactant P20, GE Healthcare). Antibodies were diluted to 10 nM in HBS-EP and concentrations of monomeric and trimeric

GP were prepared in HBS-EP between 5 and 500 nM. The latter were tested separately for each antibody in a series of sensorgram cycles, where 10 μ L of antibody was injected at 10 μ L/min followed by 90 μ L of GP at a flow rate of 30 μ L/min to generate an association phase of 180 s. After monitoring a dissociation phase of 300 s the chip was regenerated at the end of each cycle by successive injections of 10 μ L 40 mM HCl, 5 μ L 5 mM NaOH and 10 μ L 40 mM HCl. Sensorgrams provided a record of response unit difference between the test and reference flow cells. For each antibody buffer control cycles were interspersed between GP cycles to allow for drift correction; also, antibody blank cycles were run at each GP concentration to allow correction for any non-specific binding of glycoprotein.

Sensorgrams were analyzed using the BIAevaluation Software (version 4.1.1, GE Healthcare). After subtraction of respective buffer control and antibody blank cycles, kinetic parameters describing association and dissociation rate constants were determined using the Langmuir binding model. Affinity constants were calculated from the mean log K_D values determined over 5 concentrations of glycoprotein.

Thermolysin Digestion

It is known that GP proteolysis by cathepsins removes the mucin-like domain and glycan cap, and is essential for binding of GP to NPC1 receptor (Chandran et al., 2005; Schornberg et al., 2006; Côté et al., 2011; Miller et al., 2012). Thermolysin mimics cathepsins and the proteolytic activity is active at physiological pH whereas cathepsins require strongly acidic pH, which is toxic to living cells. Thermolysin (P1512; Sigma) was dissolved in HM buffer (20 mM HEPES, 130 mM NaCl and 20 mM MES and pH adjusted to 7.5). EBOV glycoprotein expressing cells (E-SIAT) were trypsinised from the flask and treated with 0.25 mg/mL thermolysin diluted in HM buffer containing 2 mM CaCl_2 for 1 hour at 37°C. Then cells were washed with PBS and passed through a cell strainer as cells tend to form clumps after thermolysin treatment. To analyze antibody binding to thermolysin treated GP, 25 μ g/mL antibody was incubated with cells for 1 h. Alexa fluor 647 conjugated anti-human IgG (A21445; Life Technologies; 1:400) was used for binding detection in FACS (Attune; Life Technologies). Antibody binding to untreated GP expressing cells handled in similar manner was done in parallel for binding comparison. Log difference of binding geometric mean fluorescence intensity was calculated. Thermolysin treatment, without prior use of trypsin, was also performed in triplicate in 96 well plates.

To confirm the complete digestion of GP by thermolysin, immunoprecipitated samples were analyzed by western blot. Using the same above conditions, MDCK-SIAT1 or E-SIAT cells were treated with thermolysin. The cells were lysed for 20 min in NP40 lysis buffer, and immunoprecipitated using antibody P6 (15 μ g/mL) and 100 μ L Protein A Sepharose (Sigma, P3391). After wash, the protein A Sepharose beads were eluted in sample loading buffer and run on 12.5% polyacrylamide gel. This was blotted onto nitrocellulose membrane, probed with biotinylated 66-3-9C antibody and developed with Extravidin-HRP (Sigma, E2886).

PCR of guinea pig tissues

Blood samples were taken in RNeasy Protect animal blood tubes (QIAGEN, UK) and samples of spleen and liver collected in RNeasy Lysis tubes (QIAGEN, UK) and stored at -80°C until processing. For processing of tissue samples, samples were thawed and homogenized through a 500 μ m mesh in a Netwell plate (Corning, UK). Tissue homogenate and blood tubes were centrifuged at 500 g to remove cellular debris. Total RNA was extracted using the RNeasy Mini Kit (QIAGEN, UK) and eluted in 50 μ L RNase-free water. An Ebola Zaire strain specific real-time RT-PCR assay was utilized for the detection of viral RNA with primer and probe sequences adopted from a published method (Trombley et al., 2010); with in-house optimization and validation performed to provide optimal mastermix and cycling conditions. Real-time RT-PCR was performed using the SuperScript III Platinum One-step qRT-PCR kit (Life Technologies, UK). The final mastermix (15 μ L) comprised 10 μ L of 2x Reaction Mix, 1.2 μ L of PCR-grade water, 1 μ L of each primer (EBOV F565 and EBOV R640 both at 18 μ M working concentration), 1 μ L of probe (at 4 μ M working concentration) and 0.8 μ L of SSIII enzyme mix. Five μ L of template RNA was added to the mastermix in order to give a final reaction volume of 20 μ L. The cycling conditions used were 50°C for 15 minutes, 95°C for 5 minutes, followed by 45 cycles of 95°C for 10 s and 60°C for 40 s with a final cooling step of 40°C for 30 s. Quantification analysis using fluorescence was performed at the end of each 60°C step. Reactions were run and analyzed on the QuantStudio Real-Time Platform (Life Technologies, UK) using software version 1.2. Quantification of viral load in samples was performed using a dilution series of quantified RNA oligonucleotide (Integrated DNA Technologies).

Histological analysis of guinea pig samples

Samples of liver and spleen were placed in 10% neutral buffered formalin for at least 21 days and processed routinely to paraffin wax. Sections were cut at 3–5 μ m, stained with hematoxylin and eosin (HE) and examined microscopically. For immunohistochemistry, sections were stained for EBOV antigen using the Leica BondMax (Leica Biosystems) and the Leica Bond Polymer Refine Detection kit (Leica Biosystems). An antigen retrieval step was included for 10 minutes using the Bond Enzyme Pretreatment kit, enzyme 3 (3 drops). A rabbit polyclonal, anti-EBOV antibody (IBT Bioservices #0301-015) (dilution 1:2000) was incubated with the slides for 60 minutes. DAB chromogen and hematoxylin counterstains were used to visualize the slides.

Gene family usage of IgG genes

The gene family usage of the variable region of the human IgG heavy- and light-chains was analyzed using IMGT/V-Quest. Phylogeny tree was drawn based on MUSCLE alignment and Neighbor joining settings using MEGA version 7.

QUANTIFICATION AND STATISTICAL ANALYSIS

For animal studies, Kaplan Meier survival curves were analyzed with the log-rank (Mantel-Cox) test using Prism 7 software (GraphPad). P values of less than 0.05 were considered significant. For neutralization, each data point is an average of duplicates from one experiment. Several data points from many experimental repeats are shown in the graph. MN titers were expressed as 50% or 90% maximal effective concentrations derived by linear interpolation from neighboring points in the titration curve. Geometric Mean Fluorescence Intensity (GMI) was quantified for FACS binding using FlowJo (Treestar).

DATA AND SOFTWARE AVAILABILITY

The sequence of some mAbs have been deposited at GenBank (GenBank: MK552329 – MK552374).